AFGL-TR-84-0154

CHARACTERISTICS AND BEHAVIOR OF ATMOSPHERIC AEROSOLS; APPLICATION TO PREDICTION OF INFRARED EXTINCTION

Ronald F. Wachtmann

Systems and Applied Sciences Corporation (SASC)
1577 Springhill Road, Suite 600
Vienna, Virginia 22180

June 25, 1984

Scientific Report No. 6

AIR FORCE GEOPHYSICS LABORATORY
AIR FORCE SYSTEMS COMMAND
UNITED STATES AIR FORCE
HANSCOM AFB, MASSACHUSETTS 02731

This report has been reviewed by the ESD Public Affairs Office (PA) and is releasable to the National Technical Information Service (NTIS).

This technical report has been reviewed and is approved for publication.

MICHAEL R. SNAPP, Major, USAF
Contract Monitor

KENNETH R. HARDY, Chief
Satellite Meteorology Branch

FOR THE COMMANDER

ROBERT A. McCLATCHEY, Director
Atmospheric Sciences Division

Qualified requestors may obtain additional copies from the Defense Technical Information Center. All others should apply to the National Technical Information Service.

If your address has changed, or if you wish to be removed from the mailing list, or if the addressee is no longer employed by your organization, please notify AFGL/DAA, Hanscom AFB, MA 01731. This will assist us in maintaining a current mailing list.

Do not return copies of this report unless contractual obligations or notices on a specific document requires that it be returned.

UNCLASSIFIED

SECURITY CLASSIFICATION OF THIS PAGE

REPORT DOCUMENTATION PAGE

1a. REPORT SECURITY CLASSIFICATION Unclassified	1b. RESTRICTIVE MARKINGS
2a. SECURITY CLASSIFICATION AUTHORITY	3. DISTRIBUTION/AVAILABILITY OF REPORT Approved for public release; distribution unlimited
2b. DECLASSIFICATION/DOWNGRADING SCHEDULE	
4. PERFORMING ORGANIZATION REPORT NUMBER(S) Scientific Report No. 6	5. MONITORING ORGANIZATION REPORT NUMBER(S) AFGL-TR-84-0154
6a. NAME OF PERFORMING ORGANIZATION Systems and Applied Sciences Corporation 6b. OFFICE SYMBOL (If applicable)	7a. NAME OF MONITORING ORGANIZATION
6c. ADDRESS (City, State and ZIP Code) 1577 Spring Hill Road, Suite 600 Vienna, VA 22180	7b. ADDRESS (City, State and ZIP Code)
8a. NAME OF FUNDING/SPONSORING ORGANIZATION Air Force Geophysics Laboratory 8b. OFFICE SYMBOL (If applicable) LYS	9. PROCUREMENT INSTRUMENT IDENTIFICATION NUMBER F19628-81-C-0042
8c. ADDRESS (City, State and ZIP Code) Hanscom AFB, MA 02731 Monitor/ Michael Snapp, Maj,USAF	10. SOURCE OF FUNDING NOS. PROGRAM ELEMENT NO.: 63707F PROJECT NO.: 2688 TASK NO.: 02 WORK UNIT NO.: AB
11. TITLE (Include Security Classification) See Reverse	
12. PERSONAL AUTHOR(S) Ronald F. Wachtmann	
13a. TYPE OF REPORT Technical 13b. TIME COVERED FROM Jun 1982 TO Jun 1984	14. DATE OF REPORT (Yr., Mo., Day) June 25, 1984 15. PAGE COUNT 76
16. SUPPLEMENTARY NOTATION	
17. COSATI CODES FIELD / GROUP / SUB. GR.	18. SUBJECT TERMS (Continue on reverse if necessary and identify by block number) Atmospheric aerosols, Infrared extinction, Relative humidity, LOWTRAN aerosol models, Aerosol model selection, Tactical decision aid.

19. ABSTRACT (Continue on reverse if necessary and identify by block number)

This report describes the characteristics of atmospheric aerosols in terms of their effect on infrared radiation extinction. The aerosol properties are described in terms of the globally uniform background aerosol component and the component of the aerosol that varies on the time scale of hours to a few days. The various atmospheric processes that influence the properties of both components are described, including production, transport and removal. This report discusses the effect of aerosol chemical composition and atmospheric relative humidity on aerosol physical properties and relates these effects to extinction of near and far infrared radiation. These various aerosol characteristics are related to the aerosol models in the LOWTRAN Atmospheric Transmittance Code. The presence or absence of the sea-salt aerosol is presented as the most important factor influencing the variability in aerosol infrared extinction. This report presents a method of selecting the most appropriate LOWTRAN aerosol model for a given situation. The method is based on airmass history analysis.

20. DISTRIBUTION/AVAILABILITY OF ABSTRACT UNCLASSIFIED/UNLIMITED ☒ SAME AS RPT. ☐ DTIC USERS ☐	21. ABSTRACT SECURITY CLASSIFICATION Unclassified
22a. NAME OF RESPONSIBLE INDIVIDUAL Major Michael Snapp	22b. TELEPHONE NUMBER (Include Area Code) (617) 861-5585 22c. OFFICE SYMBOL AFGL/LYS

DD FORM 1473, 83 APR EDITION OF 1 JAN 73 IS OBSOLETE.

UNCLASSIFIED

SECURITY CLASSIFICATION OF THIS PAGE

Block 11 Characteristics and Behavior of Atmospheric Aerosols; Application to Prediction of Infrared Extinction.

TABLE OF CONTENTS

TABLES

FIGURES

FIGURES
(Continued)

1 INTRODUCTION

The Air Force Geophysics Laboratory's LOWTRAN Model (Kneizys et al., 1980, 1983) is used to calculate atmospheric extinction in the United States Air Force Tactical Decision Aids. LOWTRAN uses a set of model aerosol profiles to represent extinction properties of various types of atmospheric aerosols. A brief description of these models follows. A more complete description is given by Shettle and Fenn (1979). LOWTRAN aerosol models include the following:

- FOG 1 characterizes very wet aerosols found in very dense fogs,
- FOG 2 describes aerosol properties in less dense fogs such as radiation fog.

The present report describes other non-fog types of aerosols that exist at relative humidities below 99 percent. The four LOWTRAN aerosol models that characterize the non-fog aerosols are the rural, urban, maritime and tropospheric models.

(1) The rural model describes the boundary-layer background aerosol found in continental airmasses. This aerosol is composed principally of sub-micrometer soil particles and products of certain natural and man-made processes occurring in continental regions. The particle size distribution in the rural model represents a concentration of particles in the size range below 1 μm and contains two modes, one at about 0.03 μm and a second mode at 0.5 μm. The number concentration in the second mode is very low (about 1.25×10^{-4} times that in the first mode).

(2) The urban model describes aerosols that include significant concentrations of particles produced in urban and industrial complexes. The urban model size distribution is identical to that of the rural model. The chemical makeup of the aerosol is that of the rural aerosol and an added component representing soot-like aerosols.

(3) The maritime aerosol model characterizes extinction by the continental background aerosol and by sea-salt particles found in maritime airmasses. This aerosol is composed of both sub-micrometer and micrometer (up to 20 μm) sized particles. The size distribution contains the smaller of the two modes in the rural model and a second mode representing the relatively large sea-salt aerosols.

the two modes in the rural model and a second mode representing the relatively large sea-salt aerosols.

(4) The tropospheric model characterizes the aerosols in very clean atmospheres and in the free atmosphere above the boundary layer. Its size distribution contains only the smaller of the two modes in the rural model; chemical composition is that of the rural model.

Table 1 presents a comparison of 8-12 μm aerosol extinction coefficients from LOWTRAN V for three of the aerosol models for a range of visibilities and relative humidities. This table also presents for comparison the molecular extinction coefficients at 8-12 μm for the same relative humidity values at two different temperatures. Fig. 1 presents the 8-12 μm transmission on a 2 km path under the indicated conditions for the three models as a function of relative humidity. The following features of these data highlight the importance of aerosol model selection:

(1) The aerosol extinction at 8-12 μm for the rural and urban models is small except at low visibilities. With moderate to high relative humidity and visibility greater than 4 km, aerosol extinction in continental aerosols is overshadowed by molecular extinction.

(2) The relative humidity response of the rural and urban models is weak. In comparison the maritime model shows a strong response at relative humidities above 70%.

(3) Aerosol extinction in the maritime model can be relatively high even with good visibilities.

Table 2 and Fig. 2 present corresponding data from three LOWTRAN VI models at 1.06 μm. Note the difference in path length and visibility between Figs. 1 and 2. Molecular extinction is negligible at 1.06 μm and is omitted from this data set. Note the following features:

(1) Relative humidity response of each of the models is low. The difference in relative humidity sensitivity is particularly striking for the maritime model in comparison to that shown in Fig. 1.

(2) The differences in 1.06 μm extinction among the models are greater at all relative humidities than the differences at 8-12 μm.

(3) Aerosol extinction is much stronger at 1.06 μm than at 8-12 μm.

Table 1. A comparison of aerosol and molecular extinction coefficients (km^{-1}) in the 8-12μm band for various visibility, relative humidity and absolute humidity values. Aerosol extinction data are given for three LOWTRAN V aerosol models.

Relative Humidity (Percent)	Aerosol Extinction (km^{-1})									Molecular Extinction (km^{-1})	
	Rural			Urban			Maritime			$T=5^{o}C$	$T=30^{o}C$
	Visibility (km)										
	2	4	10	2	4	10	2	4	10		
30	.175	.088	.035	.195	.097	.038	.223	.113	.045	.045	.141
60	.176	.088	.035	.195	.098	.038	.242	.122	.048	.073	.354
80	.177	.089	.035	.180	.090	.035	.388	.196	.078	.096	.522
90	.188	.094	.037	.185	.092	.036	.470	.238	.094	.107	.603
95	.200	.100	.039	.191	.095	.037	.569	.289	.115	.112	.665
99	.230	.115	.045	.204	.102	.040	.883	.451	.180	.119	.772

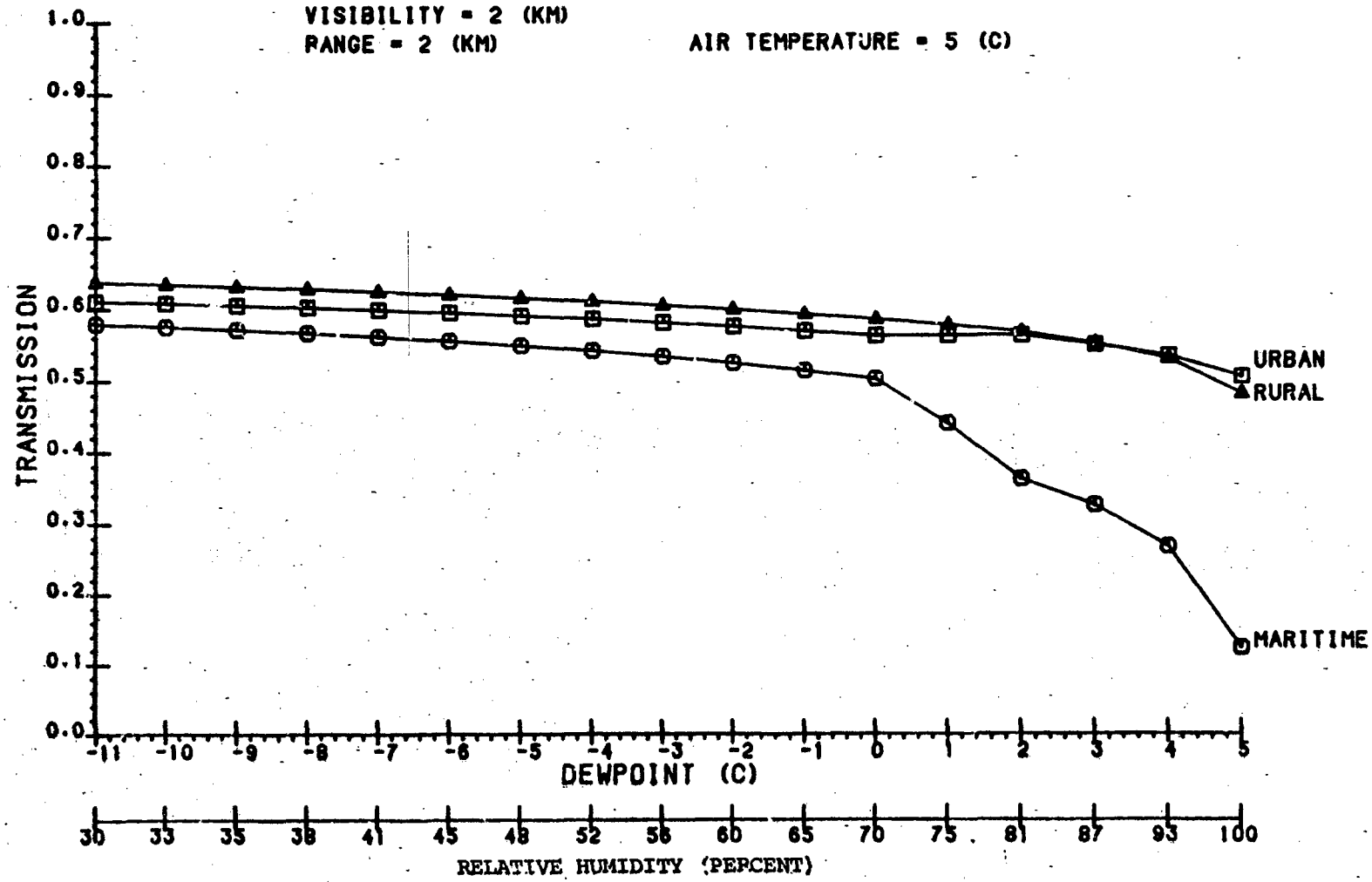

Fig. 1. 8-12 μm transmission as a function of relative humidity at 5°C for three LOWTRAN V aerosol models. The transmission values represent the combined effects of aerosol and molecular extinction.

Table 2. A comparison of 1.06μm aerosol extinction coefficients (km^{-1}) from three LOWTRAN VI aerosol models.

Relative Humidity (Percent)	Rural			Urban			Maritime		
	Visibility (km)								
	2	4	10	2	4	10	2	4	10
30	.813	.405	.159	.909	.452	.177	1.40	.696	.274
65	.816	.406	.159	.905	450	.176	1.48	.734	.288
75	.826	.411	.161	.900	.448	.175	1.58	.787	.309
93	.885	.440	.173	.952	.473	.185	1.75	.868	.340
100	.980	.487	.191	1.065	.530	.208	1.84	.915	.359

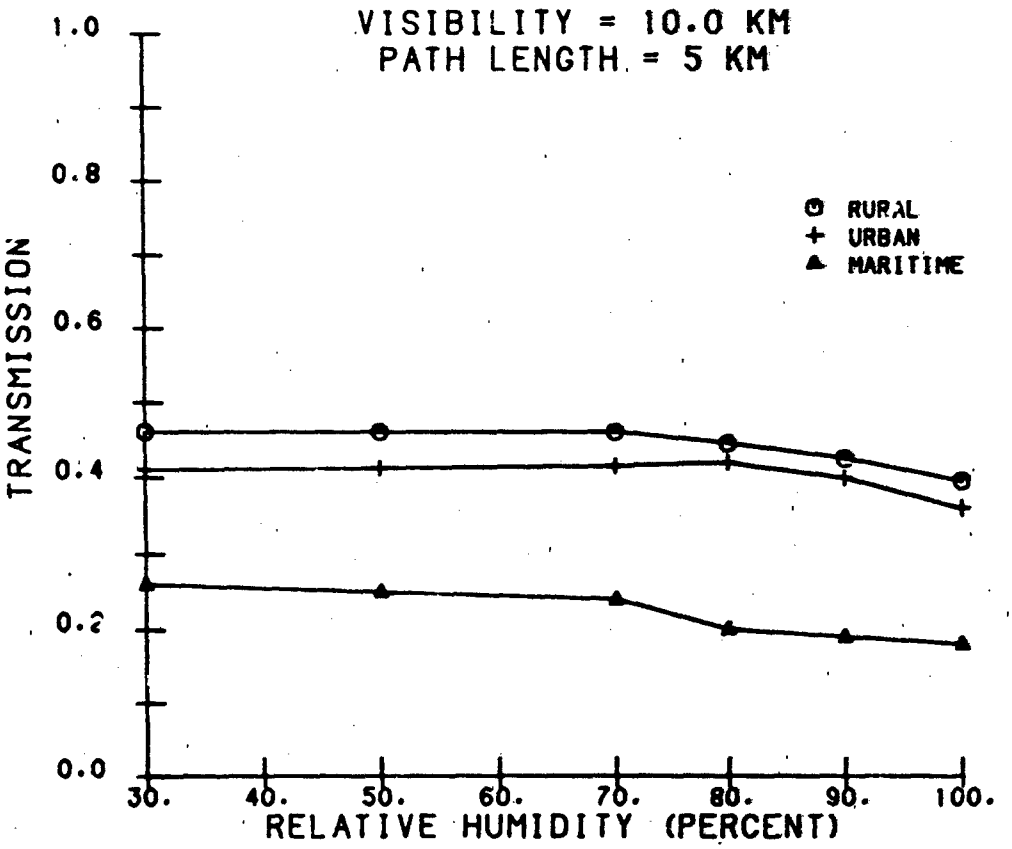

Fig. 2. 1.06 μm transmission as a function of relative humidity for three LOWTRAN

Clearly, selection of the most appropriate aerosol model plays a role in estimating atmospheric transmission in the infrared spectral region. The Aerosol Model Selection Algorithm described in Section 7 of this report was developed to give the users of Tactical Decision Aids guidelines in model selection when estimating aerosol extinction in the boundary layer. We based the algorithm on published scientific literature in a number of pertinent subject areas. This paper summarizes the scientific data used in developing the algorithm and presents the underlying rationale.

Section 2 discusses methods that are commonly used to characterize atmospheric aerosols. Section 3 presents results of three aerosol studies that describe important properties of aerosols and illustrate their spatial and temporal variability. Section 4 discusses the principal processes that

influence the spatial and temporal variability of aerosol properties. Section 5 discusses factors that determine aerosol extinction efficiency. Section 6 discusses relative humidity effects. Section 7 presents the Aerosol Model Selection Algorithm.

2 CHARACTERIZATION OF ATMOSPHERIC AEROSOLS

Three properties are important in characterizing atmospheric aerosols in the context of radiation extinction. They are the total number concentration, the particle size distribution, and chemical composition of the constituent particles in various size ranges.

The total number concentration is simply the total number of particles summed over the entire range of particle sizes. The total number concentration is a convenient parameter to represent variations in aerosol concentration when the size distribution and chemical composition are specified.

The particle size distributions in atmospheric aerosols have been found characteristically to contain three modes. The three modes are named the transient nuclei mode, the accumulation mode, and the coarse particle mode. Particle size values that define the limits of the range of mode diameter for each mode vary slightly by author. We adopt the following definitions of Willeke and Whitby (1975).

Diameter	Mode
< .06 μm	Transient nuclei
.06 μm - 2.0 μm	Accumulation
> 2.0 μm	Coarse particle

The transient nuclei mode contains the Aitken nuclei, which are composed of products of both natural and man-made processes. Examples are certain organic compounds released into the atmosphere by plants, and sulphate and nitrate compounds formed either directly during fossil fuel combustion or by chemical transformation of direct combustion products. The nuclei mode includes certain particles that act as cloud condensation nuclei. Most particles in the nuclei mode are transient, because they tend to form larger particles by coagulation. The role of aerosols in the nuclei mode in radiation extinction is very small for visible radiation and completely negligible for infrared radiation. Their small extinction cross-section (see Section 6) renders them ineffective as infrared attenuators.

The accumulation mode is so named for two reasons: (1) many of the constituents in this mode are products of coagulation of particles in the transient nuclei mode; and (2) particles in this mode tend to accumulate in a way that results in atmospheric residence times from several days to several

weeks. The small size of these particles implies low sedimentation rates; at the same time, precipitation washout of these particles is less efficient than for larger particles (see Section 4). Particles in this mode are principal attenuators of visible and near infrared radiation. Their role in middle and far infrared extinction is much less.

The coarse particle mode often contains particles as large as 20 μm in significant number concentrations. This mode includes fly-ash particles from fossil fuel combustion, airborne dust and sea-salt particles. Residence times for particles in this mode are short compared to those in the accumulation mode because of high sedimentation rates and efficient washout by precipitation. Particles in the 10-20 μm range have residence times on the order of hours, while the smaller particles (2-10 μm) typically have residence times of 1-3 days. Particles in this mode are the dominant aerosol attenuators of middle and far infrared radiation.

The distributions of particles sizes within each mode typically follow a log-normal distribution quite closely (Shettle and Fenn, 1979). The parameters required to specify the size distribution for each mode with good accuracy are the mode radius, the geometric standard deviation of particle size about the mode radius and the total number concentration in the mode. Specification of these parameters for each of the three modes enables a very accurate definition of the entire size distribution for most aerosols.

Authors sometimes describe the aerosol size distribution by estimating aerosol particle surface area or aerosol particle volume (or mass) as a function of particle size. The surface area distribution is useful in a study of radiation extinction because surface area makes more apparent the role of particle size in extinction at various wavelengths.

Figs. 3 and 4 illustrate the number distribution, surface area distribution, and volume distribution for the mean aerosol condition during October 1971 at the Denver City Maintenance Yard (Willeke and Whitby, 1975). The modes in the distribution are not obvious in Fig. 3. They are more readily seen in the distribution of surface area and volume in Fig. 4.

Variations in the strength of the individual modes are useful for the present purpose because they often directly reflect the variation in aerosol extinction in certain wavelength regions.

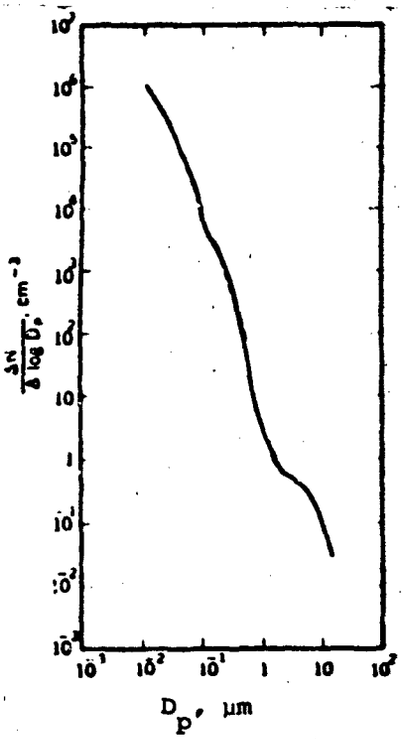

Fig. 3. The grand average of the number density distribution from October 1971 measurements of Denver's City Maintenance Yard. D_p is the particle diameter (Willeke and Whitby, 1975).

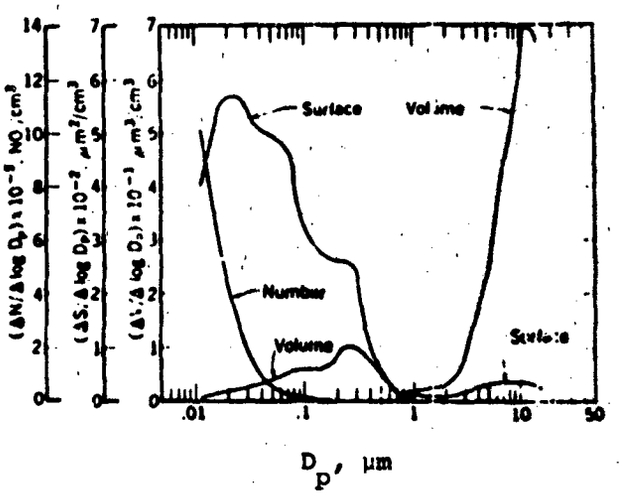

Fig. 4. Normalized frequency plots of number density, surface area and volume distributions for the grand average October 1971 measurements of Denver's City Maintenance Yard. Note the bimodal distribution of volume and the fact that each curve shows features of the distribution not shown by the other plots (Willeke and Whitby, 1975).

The chemical composition of the aerosol is important in radiative transfer processes in three ways. The first is the dependence of the complex refractive index on this property. Secondly the chemical composition is directly related to the sources and mechanisms for production of the aerosol. These are important in understanding the observed temporal and spatial distributions and the particle size distributions of various types of aerosols. Thirdly, the chemical composition determines the response of the aerosol to changes in relative humidity.

The chemistry of aerosols may be classified in three ways, namely, soluble or insoluble, organic or inorganic, and by source, particularly whether the source is natural or related to human activity. Solubility is perhaps the most important of these because it determines the aerosol's response to changes in relative humidity. Examples of soluble aerosol compounds are ammonium sulphate, nitric acid and nitrate salts, sulfuric acid and sodium chloride. Insoluble aerosol compounds include elemental carbon (soot), soil-derived aerosols such as sub-micrometer clay particles and much larger particles due to wind-blown dust, and other aerosols due to human activity such as fly ash. The behavior of soluble aerosols will be treated in Section 6 on relative humidity effects.

3 DESCRIPTIVE CASE STUDIES

In this section we present descriptive aerosol data from three research programs. These data were selected because they describe many of the aerosol properties pertinent to infrared extinction, provide information on temporal and spatial variability, and describe certain processes that influence the space/time distribution of aerosol properties. Case I presents a global view of aerosol distributions and illustrates how aerosol properties differ among various airmass types. Case II presents data on the marine aerosol and includes a study of the behavior of windblown dust. Case III describes the behavior and characteristics of certain urban aerosols.

Case I Global Monitoring Station Data

Bigg (1980) published a comparison of the aerosol characteristics at four global baseline atmospheric monitoring stations. The stations are to establish reference levels of atmospheric constituents that may affect global climate. The data from these stations were found useful for our purpose because features of the aerosol at each station and the differences among them illustrate many pertinent features of aerosol variability.

The four stations were Point Barrow, Alaska; Mauna Loa Observatory, Hawaii; Cape Grim, Tasmania; and a South Pole station. Table 3 provides descriptive site data. Periods of observation at each site are indicated, along with a brief description of certain pertinent meteorological conditions.

Fig. 5 shows representative number density versus particle size for the aerosol at each of the four sites. Fig. 6 is a similar plot of the mass distribution. Note the following features of Fig. 5.

(1) Number densities in the size range from 0.03 μm to 0.08 μm are quite similar among the four stations. Bigg reported that the size distribution of the aerosol varied little with time at Point Barrow. He found that the predominant chemical constituents in the small particle component at Point Barrow were sulferic acid and ammonium sulfate. He attributed the relatively high number concentrations above 0.2 μm to a sea-salt component. He postulated that the small particles were transported poleward from mid-latitude regions by the high-altitude circulation. The uniform number densities of the small particles and the remote origin of the small particles at Point Barrow demonstrate the permanence and long residence time of the small particle

Table 3. Descriptive site data on the four atmospheric monitoring stations as reported by Bigg (1980).

Station	Latitude	Elevation (meters)	Topographic Features	Observation Period(s)	Meteorological Conditions
Point Barrow	71°N	Sea Level	Flat ground; frozen sea; snow covered land	Dec 76-Mar 77 Mar 78-May 78	Winds predominantly E-NE ∿ 5-10 m sec^{-1}
Mauna Loa	19°N	3400	Flank of a huge, gently sloping volcano; peak at ∿4000 m	Jun-Jul 75 Jun-Jul 76	Dominated by local thermal effects; downslope SE winds at night; upslope N winds in afternoon
Cape Grim	41°S	∿100	Edge of 90m cliff, NW coast of Tasmania; on the highest point in the area.	Continuously since Apr 76	The "roaring forties"; winds W-S > 10 m sec; frequent showers in winter; monitoring site protected from sea spray by terrain
South Pole	90°S	2850	High plateau; highest point on the plateau ∿4000 m.	14-28 Jan 79	Unknown

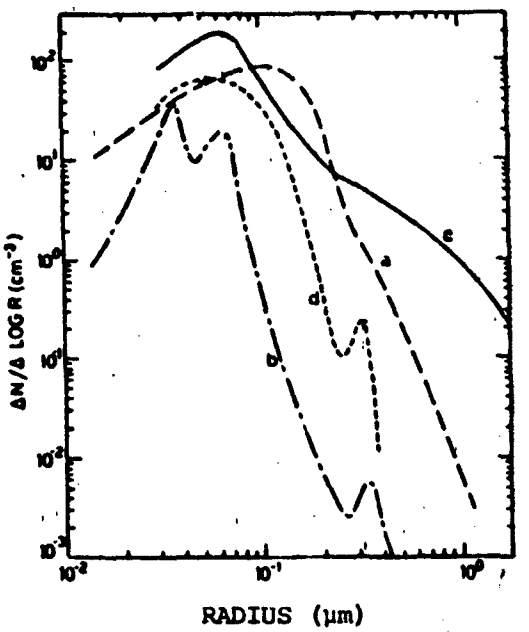

Fig. 5. The number density distributions of particles at (a) Barrow, Alaska, (b) Mauna Loa, Hawaii, (c) Cape Grim, Tasmania and (d) South Pole (Bigg, 1980).

component and indicate a more or less steady-state global production mechanism. Sulfur compounds dominated the South Pole aerosol with a much smaller sea-salt component. Bigg attributes the origin of the South Pole aerosol to mechanisms similar to those ascribed to the Point Barrow aerosol. The low concentration of particles above 0.2 μm at the South Pole may be due to washout by precipitation or to the high elevation of the site.

(2) Particle concentrations in the Mauna Loa aerosol were low at all particle sizes above 0.1 μm. This result differs perhaps from the type of aerosol expected in a maritime location. Absence of the large particles is due to the high elevation of the Mauna Loa site and the inhibiting effects of the trade wind inversion on vertical transport of large particles. The Mauna Loa aerosol features are characteristic of aerosols often found in the troposphere above the boundary layer. Junge (1972) reported similar features in aerosols above the boundary layer in the North Atlantic. The chemical composition at Mauna Loa was similar to that of the high latitude aerosols, with a predominance of water soluble sulfur compounds.

(3) The distinctive feature of the Cape Grim aerosol is the high particle count in the size range above 0.2 μm. Note that in Bigg's study, the upper size limit of distributions reported is about 1 μm. Since the Cape Grim aerosol is clearly a marine aerosol, it is reasonable to assume that signifi. ant number concentrations would be found for particles as large as 20 μm. The small particle component of the Cape Grim aerosol was dominated by sulfur compounds. The large particle component was almost entirely sea salt.

The particle mass distribution plotted in Fig. 6 shows several important features. Note the concentration of mass in very small particles in the Mauna Loa aerosol. The mass is distributed among larger particles ranging from .04 μm to 0.5 μm for the Point Barrow and South Pole aerosols. The Cape Grim aerosol shows a large mass distribution at much larger

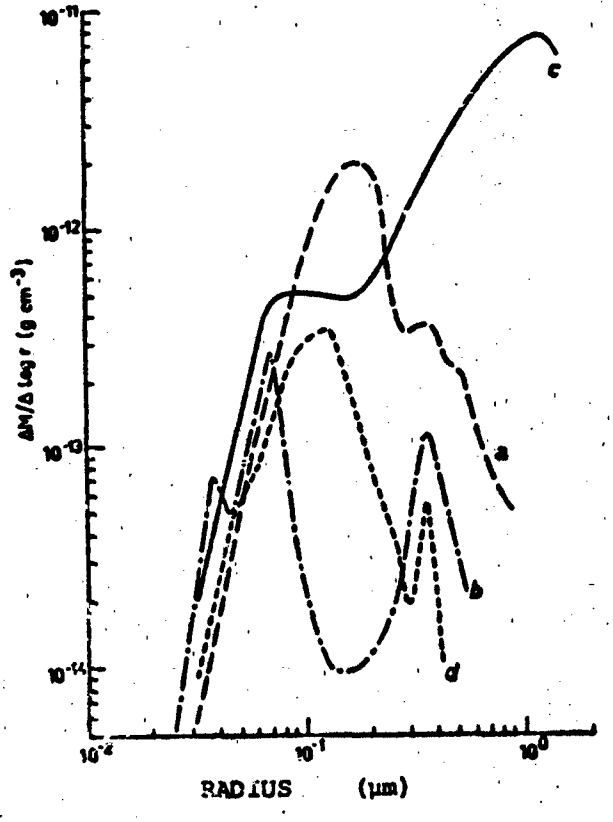

Fig. 6. The mass distributions of particles at (a) Barrow, Alaska, (b) Mauna Loa, Hawaii, (c) Cape Grim, Tasmania and (d, South Pole (Bigg, 1980).

particle sizes. A significant mass concentration at Cape Grim is likely above the measurement size limit at 1 μm. Bigg estimated the total mass concentration (integrated over particle sizes to 1 μm) as follows:

Mauna Loa	.08 μg m^{-3}
Point Barrow	0.8 μg m^{-3}
South Pole	0.14 μg m^{-3}
Cape Grim	3.7 μg m^{-3}

The particle size distributions and mass concentrations at three of these stations clearly permit classification of their aerosols according to the LOWTRAN models as follows:

Mauna Loa	Tropospheric
Point Barrow	Rural
Cape Grim	Maritime

The South Pole aerosol falls between the rural and tropospheric models.

Another important feature of Fig. 6 is the modal distribution of the aerosol mass. The Mauna Loa aerosol shows two modes, but both are in the small-particle component. The Point Barrow and South Pole aerosols show a weak secondary mode near 0.4 μm. The Cape Grim aerosol clearly shows both the accumulation mode and the coarse-particle mode. In this case, the small-particle mode represents the stable aerosol with a continental origin, while the coarse-particle mode represents the sea-salt aerosol.

Figure 7 shows electron microscope photographs of aerosol samples taken at the four sites. These photographs clearly show the different size distributions among the aerosols.

Case II North Atlantic Data from the R. V. Meteor

Junge and Jaenicke (1971) and Junge (1972) contain reports of the voyage of the German ship R. V. Meteor in the North Atlantic in 1969. Fig. 8 is a map of the expedition. Extensive aerosol measurements were taken on the northbound leg of the voyage from April 14 to May 7. The ship crossed the Intertropical Convergence Zone (ITCZ) on the northbound leg on April 17th. The airmass south of the ITCZ was considered maritime in character. The airmass immediately north of the ITCZ had its origin in the Sahara desert and was laden with Sahara dust.

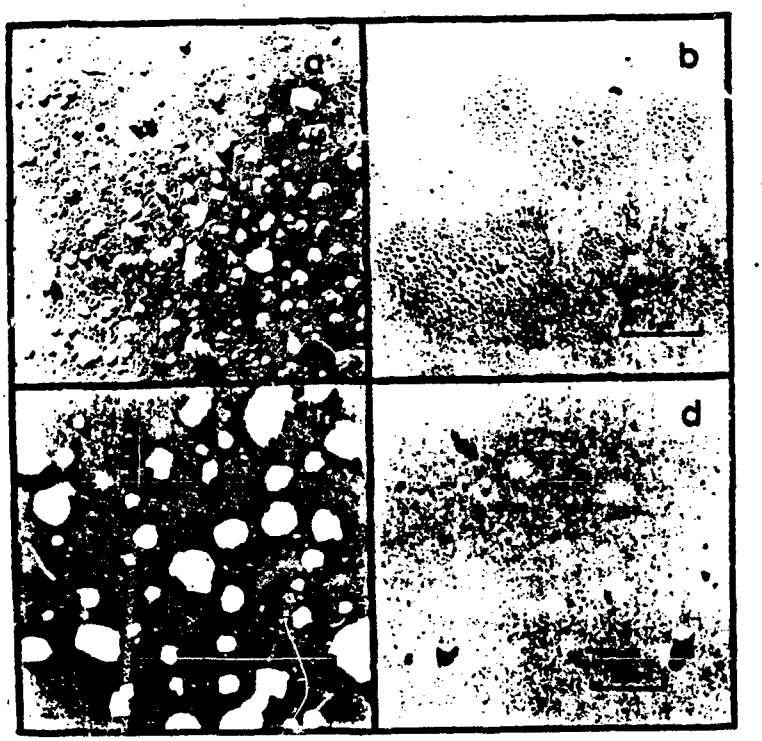

Fig. 7. Particles collected with 1 mm jet impactor at (a) Barrow Alaska, (b) Mauna Loa, Hawaii, (c) Cape Grim, Tasmania and (d) South Pole. The fields of view shown correspond roughly to 100 cm^3 of sampled air. The inset is 2 um in length (Bigg, 1980).

The visual range was recorded at the green wavelength (0.55 μm) with a specially designed instrument. Traces from this device indicated a reduction in visual range from 100 km to 20 km upon crossing the ITCZ. The authors reported that dust was deposited on the ship's deck after crossing the ITCZ. Further north, the airmass returned to a purely maritime character on about April 24. Fig. 9 shows a twice daily analysis of the trajectory of the airmass observed at each point on the northbound leg after crossing the ITCZ. Successive dots on each trajectory represent estimated 12 hour airmass movement.

Fig. 10 shows time traces of the output from various instruments aboard ship. The instruments are named and their output is described in the caption. The following features of the traces provide insight into the variation of several aerosol properties.

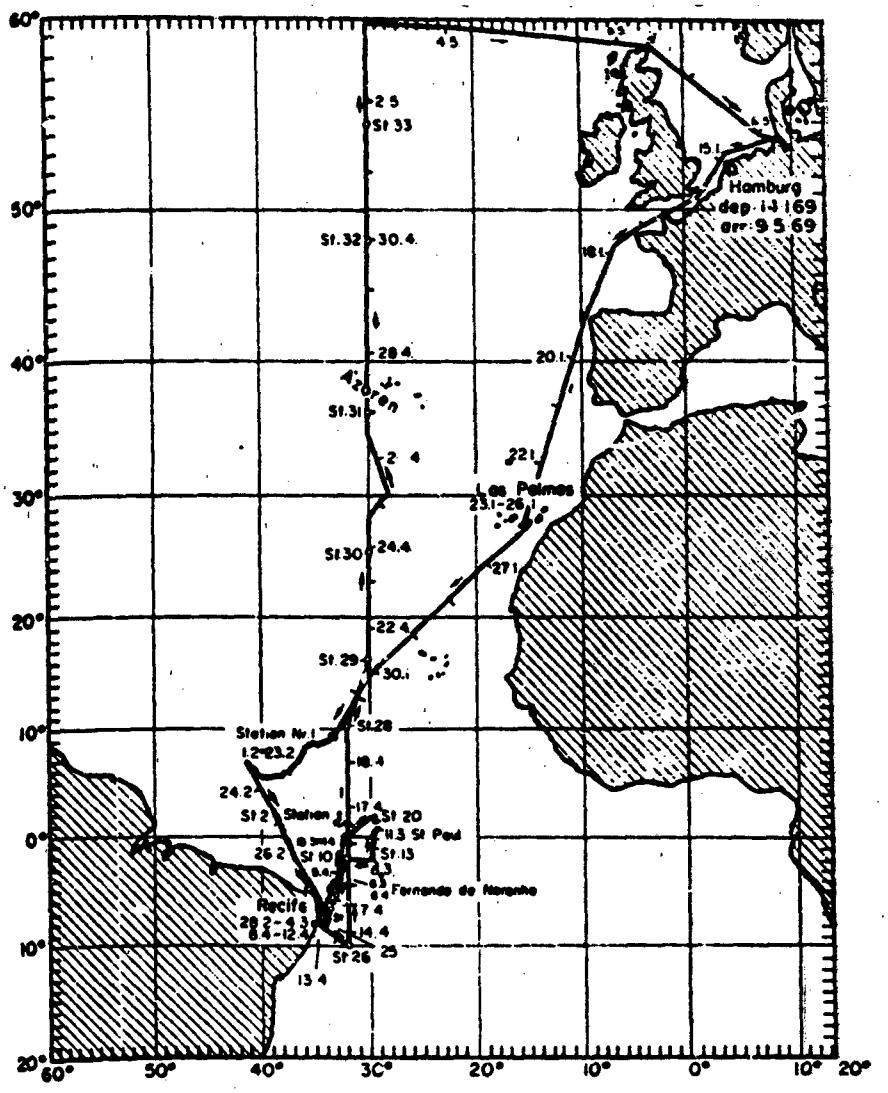

Fig. 8. Map of the Atlantic expedition of the German Research Vessel Meteor, Spring 1969. Dates are indicated at various positions in the expedition by day.month (Junge and Jaenicke, 1971).

Trace A shows total counts of the Aitken nuclei in the range .001 μm to .01 μm. Note that the number concentration varies little with airmass changes, with a mean value about 600 cm^{-3}. The authors reported surprise at the steady values and their unexpectedly high magnitudes. These data were the first real evidence of a steady state production mechanism to offset the loss of particles in this size range through coagulation. The authors

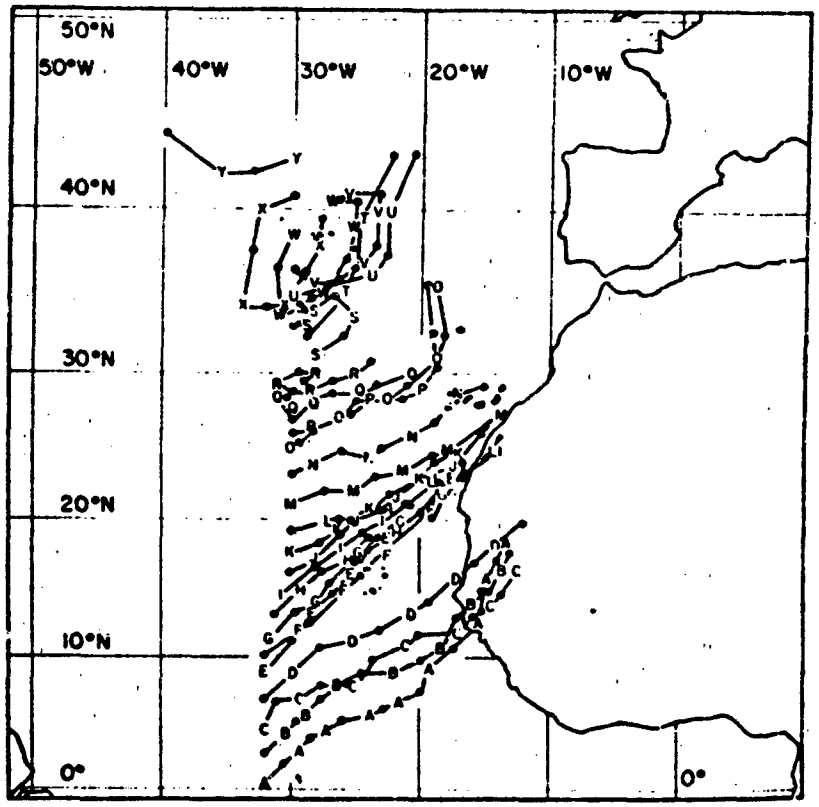

Legend

A,B	17.4.1969	M,N	23.4.1969
C,D	18.4.1969	O,P	24.4.1969
E,F	19.4.1969	Q,R	25.4.1969
G,H	20.4.1969	S,T	26.4.1969
I,J	21.4.1969	U,V	27.4.1969
K,L	22.4.1969	W,X	28.4.1969
		Y	29.4.1969

Fig. 9. Trajectories of the air masses in steps of 12 hr. The letters indicate the time of arrivel (in GMT) at midnight and noon respectively by day.month.year in the legend. Continental air masses are from A to M, marine air masses from O to Y (Junge and Jaenicke, 1971).

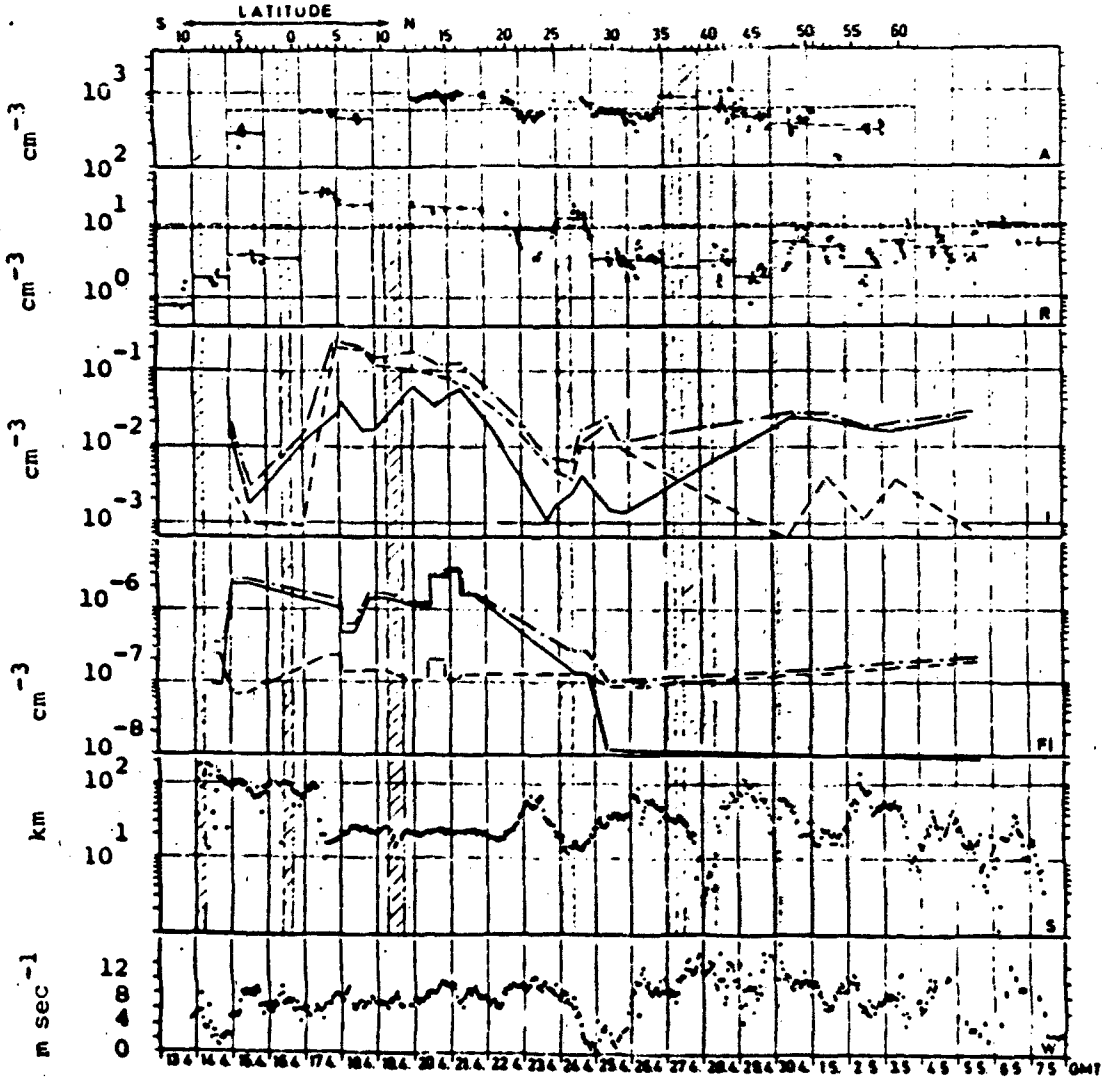

Legend

A : Aitken condensation nuclei

R : Royco particle counter (radius > 0.3 µm)

I : Single stage impactor (radius > 3 µm)

FI : Rotating Impactor (radius > 19 µm)

S : Visibility with green wavelength

, : Wind speed

For I and FI

____ Soluble particles

_ _ Insoluble particles

__.__ Sum of both

Fig. 10. Particle concentrations measured with various instruments as a function of time (GMT) and position of the ship on 30° W. Hatched areas indicate wind direction 80° - 120° relative to main ship axis with high probability of pollution from the ship (Junge and Jaenicke, 1971).

considered this nuclei count as low, however, compared to those found in continental regions.

Trace R represents total number concentrations in the range of particle sizes above 0.3 μm. Note the sharp increase in number concentrations on April 17 upon moving into the Saharan airmass. This increase in number concentration is clearly the cause of the simultaneous reduction in visibility as shown in Trace S. Number concentrations in this size range returned to much lower levels on April 24 when the ship again entered an airmass with a long maritime history. The subsequent mean value of visibility was significantly higher than that observed in the Saharan airmass but was also quite variable. The variation shows a strong inverse correlation with the number concentrations in Trace R.

Trace I represents total number concentrations for particle sizes greater than 3 μm. This trace shows the counts separately for the soluble and the insoluble components. Trace I shows a sharp increase in the counts upon entry into the Saharan airmass on April 17, with most of the increase in the insoluble component (dashed line). These are the Sahara dust particles. Upon entry into the maritime air on April 24 the total particle count in the range above 3 μm decreased markedly. The counts for the insoluble component decreased by almost a factor of 100. The soluble component dominated the distribution after April 25 with counts about the same as those found for the soluble component before that date.

Trace FI shows that the number concentrations of particles above 19 μm are three to four orders of magnitude lower than the counts of particles above 3 μm. Because of their low number density, their existence in the undisturbed marine aerosol is of no consequence to the strength of infrared extinction. We refer the reader to the source paper for a discussion of the properties of these very large aerosols.

Junge reported a detailed analysis, based in part on the R. V. Meteor data, of the behavior of sea-salt aerosols in the marine environment. The following are pertinent conclusions of his analysis:

(1) The upper limit of the size distribution is 20 μm in the sea-salt aerosol. He concluded that particles larger than 20 μm would not be found in significant numbers except in the layer (on the order of 10 meters thickness) immediately above the ocean surface. The particles larger than 20 μm are produced by sea spray and are lost rapidly by sedimentation.

(2) The lower size limit of sea-salt particles is about 0.1 μm. Although their number concentrations may be quite high in the size range from 0.2 μm to 1.0 μm, their counts are an order of magnitude less than those of other soluble compounds in the background aerosol in this size range.

(3) The chemical composition of sea-salt particles is dominated by sodium chloride. However, significant amounts of other soluble and insoluble compounds are found within the sea-salt crystals.

(4) Particle counts decrease rapidly with height above about 0.5 km over the ocean, with practically no sea salt found above 2-3 km. This finding does not necessarily hold over land because vertical transport mechanisms operate more effectively over land.

(5) Residence times for sea-salt particles in the size range below 10 μm average about three days. The particles above 10 μm will have shorter residence times. Residence time depends both on sedimentation and on rain-out and washout.

Junge's work represents one of the early efforts to understand the global background aerosol. He found that the composition of the background aerosol, except for the sea-salt component, was very uniform in both the horizontal and the vertical in oceanic regions. He reached the tentative conclusion that sulfate compounds made up more than 50 percent of these aerosols. The data presented by Bigg in Case I are results of just one of several later research programs that have confirmed his findings.

Junge found that the principal constituent of the global background aerosol is ammonium sulphate These particles are known to have a continental origin. Their number concentrations dominate the particle distribution in the size range from 0.05 μm to 0.5 μm. Fig. 11 shows the relationships between the continental and marine aerosols in this size range.

Case III Urban Aerosols

Willeke, et al. (1974) and Willeke and Whitby (1975) are reports of extensive studies of urban aerosols in the Denver, CO area, as well as measurements at a number of other locations. Measurements were taken at two different locations in the Denver area in the fall of 1971. Willeke and

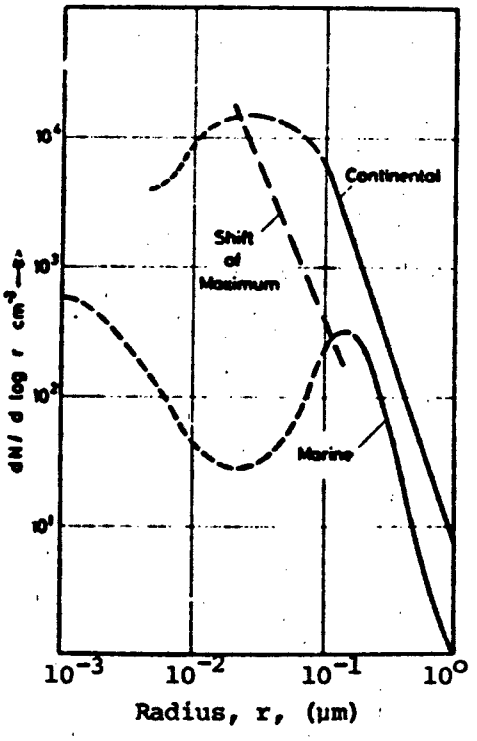

Fig. 11. Idealized size distributions of continental and marine aerosols. (Adapted from Junge, 1972).

Whitby compared these measurements to those obtained at other locations during the period from 1969-74. All measurements were taken with the Minnesota Aerosol Analyzing System (MAAS). Their results represent several thousand in-situ measurements of aerosol particle size distributions. Findings pertinent to the problem of visible and infrared extinction are presented here.

The MAAS measures particles in the size range from .0075 μm to 17.5 μm diameter. Surface area distributions were computed by assuming a spherical shape for the particles. Visual range was determined from nephelometer measurements of the scattering coefficient in the visible spectrum.

Fig. 12 shows aerosol particle surface area distributions as a function of particle size under five different conditions. Table 4 lists a number of key parameters for these five cases.

Variation in the visual range in the various types of aerosols is a matter of interest here. In the five aerosol data sets presented

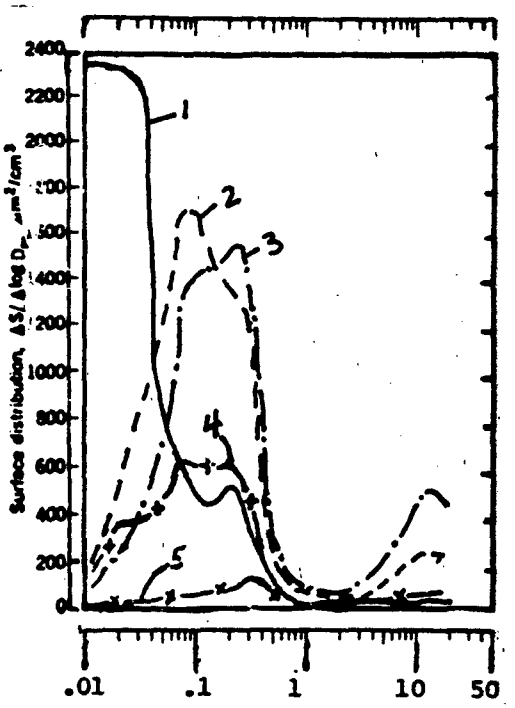

Legend

1 —— Moderate urban pollution plus heavy traffic. Denver, CO; 2½ km West of downtown, Oct. 26, 1971, 1640-1700 hours.

2 – – – Heavy urban pollution. Denver-Welby, CO; 10km NE of downtown; Nov. 9, 1971, 0700-0900 hours.

3 —·— Heavy urban pollution. Denver-Welby, CO; 10 km NE of downtown; Nov. 9, 1971, 0920-1330 hours.

4 —+— Urban district background plus anthropogenic Denver-Welby, CO; 10 km NE of downtown; 0200- 0400 hours.

5 —X— Average western continental background. Fort Collins, CO; Aug. 13-14, 1970.

Fig. 12. Aerosol surface area distributions under the five conditions described in the legend. This figure was adapted from data presented by Willeke and Whitby. The plots for distributions 4 and 5 are indistinguishable beyond a diameter of 0.5 μm in this presentation (Willeke and Whitby, 1975).

Table 4. Key parameters for five cases from Willeke and Whitby (1975). Case numbers on the left side correspond to those in Fig. 12. The right hand side contains data for other cases, with size distributions similar to those of the corresponding cases on the left-hand side. The visual range datum opposite Case 1 was reported in the Case 1 data. The remaining values of visual range were contained in data for the three "other cases."

Case	Nuclei Mode (Aitken Count) (cm^{-3})	Total Aerosol Volume ($\mu m^3/cm^3$)	Sub-Micrometer Volume ($\mu m^3/cm^3$)	Total Surface $\mu m^2/cm^3$	Location	Date	Conditions	Visual Range (km)
1	2300K	37	18	2100				19.8
2	500K	260	36	1890	Pomona, CA	24 Oct 74	Urban Pollution	6.1
3	425K	470	39	1780				
4	214K	66	16	762	Mojave Desert	4 Nov 72	Urban District Background	23.5
5	2.3K	30	2.5	85	Mojave Desert	1-2 Nov 72	Average Continental Background	78

in Fig. 12, only the first included a report of visual range. In order to obtain comparative data on visual range, additional cases reported by Willeke and Whitby were analyzed in search of comparable size distributions accompanied by visual range data. The right hand side of Table 4 contains data for three cases containing reports of visual range. The size distribution in each of these three cases was very similar to that of the corresponding case(s) on the left side of the table.

Note from Fig. 12 that in most urban aerosols, the particle surface area distributions are several orders of magnitude higher, in some subrange below 0.5 μm, than corresponding values in the continental background aerosols. The specific subrange in which this occurs depends on the nature, source and age of the pollutants and has a direct bearing on the effect of the urban aerosol on visual range.

We note that in Case 1, the visual range is not appreciably less than in Case 4, in spite of the very high particle surface area in the subrange below 0.1 μm. The small particles in this subrange are not efficient attenuators of visible light. Cases 2 and 3 show a visual range much lower (deduced from the Pomona, CA data) than that reported in Case 1. We will show in Section 5 why the small particles in Case 1 have little effect on the visual range.

Note that the size distributions in Fig. 12 show that Cases 1 and 4 have similar number concentrations in the size range from 0.1 μm to 1.0 μm. The visual range values are similar in these two cases. In fact, the similar values of visual range reflect the similarity of particle counts in the size range that controls visibility restriction. The numerous particles in the nuclei mode in Case 1 had a small effect on visibility.

The downtown Denver site is located about 100 meters from a freeway. Note that the period for Case 1 was during evening rush hour traffic. The observation site was downwind from the freeway in a brisk 30 km hr^{-1} wind. The particle size distribution below 0.1 μm represents fresh combustion aerosols generated in the freeway traffic. Vehicular traffic in the City Maintenance Yard had subsided for the day, and few power plant emissions reached the site; hence the particle counts in the range above 1 μm were very low.

The high value of surface area distribution below 0.1 μm in Case 1 is a transient feature. Within one or two hours, the Aitken nuclei coagulated and formed another peak in the distribution around 0.1 μm. Case 2 illustrates the distribution measured on another date at a site located some 6-7 km from the nearest freeway. This distribution is similar to that expected from Case 1 after the coagulation process has acted for a few hours. Case 3 represents further aging of a similar aerosol, just two hours after Case 2 at the same location. These temporal patterns are characteristic of heavy urban pollution.

The coarse particles at 10 μm in Cases 2 and 3 are unrelated to the fine particles. These particles were attributed to settling out of fly ash from power plants.

Case 4 is a surface distribution characteristic of the urban district background. This represents a condition of aged aerosols in which dispersion has decreased the number concentrations. This distribution shows two peaks. The peak at 0.08 μm represents the coagulation of fresh nuclei, while the second peak represents the remains of older aerosols.

4 PROCESSES AFFECTING THE NATURE OF THE AEROSOL

The total mass content of aerosol in the atmosphere and its variation in time is determined by production and loss. The spatial distribution of the aerosol, its chemical composition, and its size distributions are determined by various processes. This section discusses some processes of importance to the problem of selecting an appropriate aerosol model.

Fig. 13 summarizes the definitions of the particle size ranges for the three modes commonly found in aerosol size distributions. It identifies the principal aerosol sources and characterizes the residence times typical of the aerosols in each mode.

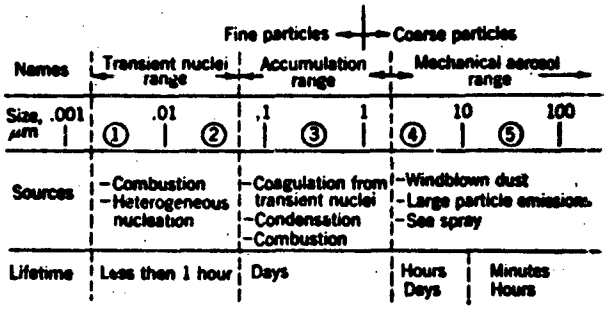

Fig. 13. Nomenclature, origin, lifetimes, and sizes of aerosols that contribute to the three modes observed in the atmosphere. Size ranges refer to particle diameter. (Willeke and Whitby, 1975)

Production Processes

We may classify aerosol production mechanisms according to the time scale on which they influence the atmospheric aerosol. The time scale of interest to us lies in the range of a few hours to a few days. Many important production processes affect the aerosol on a much longer time scale. Their products form the global background aerosol with rather uniform spatial and temporal characteristics. From our perspective these processes act as more or less steady state sources for maintenance of the background aerosol. Their products are represented in LOWTRAN by the rural aerosol model in the boundary layer and by the tropospheric aerosol model in the atmosphere above the boundary layer. The following are the principal processes that maintain the background aerosol.

- Fossil fuel combustion and forest fires produce global background aerosols principally in the nuclei range. Certain aerosols in the accumulation range are also direct products of combustion. The aerosols in the nuclei range coagulate rapidly to form aerosols in the accumulation range. Both direct and indirect products have long atmospheric residence times. These processes are the origin of many of the sulfur, nitrogen and carbon compounds in the background aerosol.

- Plant emissions produce aerosols in both the nuclei and accumulation ranges. Certain organic aerosols and nitrogen compounds result from this source. The product of these emissions is often seen as blue haze in regions of extensive vegetation.

- Sea spray and sea foam produce aerosols across a wide size range. Those in the range below 0.3-0.5 μm become a part of the background aerosol. Their number concentrations in this size range are much lower, however, than those of aerosols from other sources.

Certain production processes result in significant variability in aerosol properties on the time scale of hours to days. The following are the principal mechanisms of interest to our forecasting problem.

- Fossil fuel combustion in urban and industrial complexes produces short term local variability. Aerosols result in all three size ranges. Those in the nuclei and accumulation ranges ultimately enter the background aerosol. Large particle emissions, such as fly ash, are strongly influenced by sedimentation and by precipitation scavenging. As a result, they exhibit short residence times.

- Sea spray and sea foam are the primary production mechanism for sea-salt particles. Those in the size range from 2-5 μm exhibit residence times of a few days. The larger sea-salt particles (above 10 μm are removed by sedimentation on the time scale of a few hours. Fig. 14 is taken from data published by Wells et al (1977). They show the dependence of coarse particle concentrations in maritime air on wind speed. The very large particles (above 20 μm) in these distributions are found only in a shallow layer (on the order of 10 meters in depth) above the ocean surface. They remain airborne for time periods of less than a few hours because of sedimentation. The depth of the marine aerosol layer (for particles smaller than 20 μm) depends on the strength of vertical turbulent mixing.

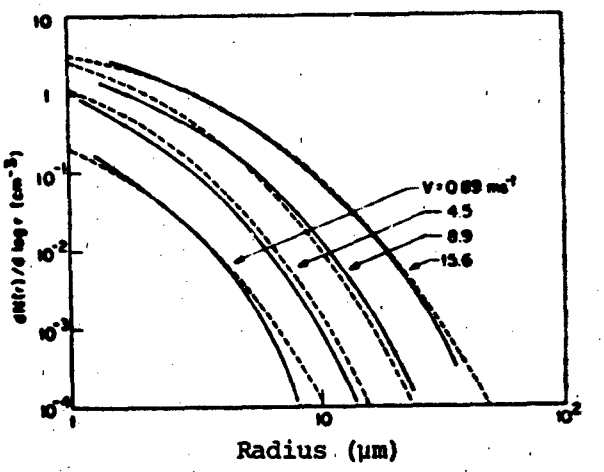

Fig. 14. Characteristic aerosol number density distributions in maritime air as a function of velocity for a RH of 80 percent (solid lines). Predictions of the maritime component of the Wells model based on these data are also shown (dotted lines)(Wells, 1977).

The sea-salt aerosol is of primary importance in forecasting infrared extinction. The size of the sea-salt particles and their response to changes in relative humidity are the largest overall source of time/space variability in the large particle concentrations. An estimate of their relative concentration is quite important in prediction of aerosol extinction. The behavior and importance of the sea-salt aerosol will be discussed more in Sections 5 and 6.

Transport and Diffusion

Transport and diffusion are both effective mechanisms in redistributing the aerosol mass. Long-range transport of the small particles in the accumulation mode accounts for the globally uniform background aerosol. Transport also plays an important role on the time scale of hours to days in carrying the sea-salt in maritime airmasses into continental regions. The effect of transport of the aerosol into a region is counterbalanced in both cases by mechanisms that remove the aerosol from the atmosphere. Transport is important over short time/distance scales in relocation of urban aerosols downwind from their source.

Diffusion plays an important small-scale role in the redistribu-

tion of urban aerosols. The general effect of diffusion is to decrease their number concentrations. Vertical diffusion acts to carry urban aerosols into the free atmosphere for rapid dispersion. Horizontal diffusion acts to reduce their number concentrations while it increases their area of influence.

Removal Mechanisms

Three principal mechanisms for removal of aerosols are sedimentation, rainout and washout. Sedimentation acts to a small degree on the accumulation mode. However, its greatest importance is in the removal of large particles.

Kasten (1968) presented equations for falling speed of aerosol particles. His development considered only gravitational, viscous, and buoyant forces. From his equations, the terminal falling speed of an aerosol particle in the size range from 1 μm to 10 μm is given by the relation:

$$w = a \rho_p r^2.$$

where w is the falling speed, a is a proportionality constant, ρ_p is the density of the particle and r is particle radius. This relation shows that sedimentation rapidly becomes more effective with increasing particle size, and falling speed is directly proportional to particle density.

Junge (1972) performed an extensive analysis of expected residence times of sea-salt aerosols over the ocean. He based his study, in part, on data by Eriksson (1957), who studied the balance between sea-salt aerosol production and loss by sedimentation. Data are presented in Table 5, with expected residence time as a function of particle mass. We have converted particle mass to equivalent diameter for three different particle densities.

Eriksson's first estimate is based on gravitational fall velocities alone. The data show very long residence times for particles in the range 1-2 μm. Eriksson revised this estimate to reconcile the estimated residence time with sea-salt production estimates and observed sea-salt concentrations. Junge concluded from

Eriksson's estimates that sedimentation could not be the primary removal mechanism for particles smaller than 10 μm diameter. He did conclude that for particles larger than 10 μm, sedimentation acting alone would result in residence times considerably less than one day. He attributed the short residence times observed for the smaller particles to removal by rainout and washout.

Table 5. Estimates of residence times for sea-salt particles as a function of particle mass. The equivalent diameters are my values calculated by assuming spherical particles with a density of 2.1 gm cm^{-3} (dry sodium chloride), 1.3 gm cm^{-3} (sodium chloride in solution, and 1.0 gm cm^{-3} (pure water). (Junge, 1972, Eriksson, 1957)

Mass (grams)	10^{-12}	10^{-11}	10^{-10}	10^{-9}
	Residence time (days)			
Eriksson's estimate (sedimentation alone)	82	16	0.6	0.5
Eriksson's estimate (production and sedimentation)	3.5	1.0	0.6	0.5
Junge's estimate (see text)	1.9	1.6	1.0	.26
Equivalent diameter (μm)				
Density = 2.1 gm cm^{-3}	1.4	3.0	6.5	14
Density = 1.3 gm cm^{-3}	1.7	3.6	7.7	17
Density = 1.0	1.8	3.9	8.4	18

Rainout occurs when aerosol particles act as cloud condensation nuclei and subsequently fall out in precipitation. Washout occurs when falling precipitation particles pick up aerosol particles during their

fall. Precipitation scavenging usually refers to washout; however, in field measurements of precipitation scavenging, it is often difficult to separate the effects of rainout from those of washout.

Several theoretical studies have shown the theoretical washout efficiency of precipitation. This efficiency is a complex function of both the aerosol size distribution and the raindrop size distribution. We present one set of theoretical results to illustrate the important features.

Dana and Hales (1976) studied the theoretical dependence of washout efficiencies on both aerosol and raindrop size distributions. Fig. 15 shows the principal features pertinent to radiation extinction. Note that both axes are a logarithmic scale. Collection efficiency curves are shown for two raindrop size distribution in which it was assumed that all raindrops were the same size. Fig. 15 contains three regions in the aerosol size spectrum that represent three different aerosol collection processes. In the region below 0.05 μm collection occurs by Brownian diffusion. From 0.05 μm to about 1 μm collection occurs by impaction. This process consists of inertialess flow in which the aerosol particles are assumed to be deflected by the airstream around the raindrop. In the region above 1.0 μm, collection occurs in inertial flow in which it is assumed that aerosol particle position is unaffected by the airstream around the raindrop. We find three noteworthy features in Fig. 15: (1) very high collection efficiencies above 1 μm; (2) minimum in collection efficiency around 0.05 μm. (3) Collection efficiences much higher (about two orders of magnitude) for the large particles than for the small particles.

Radke et al. (1980) report the results of measurements of aerosol washout in various locations. Table 6 lists descriptive data on the measurement program. Fig. 16 and 17 show aerosol size distributions at two sites before and after a rain shower event. Note the well defined minimum in the washout around 0.5-0.8 μm particles diameter in both cases.

Fig. 18 shows collection efficiency as a function of aerosol particle size for each event listed in Table 6. Note that the vertical coordinate in Fig. 18 represents the percentage of particles removed by scavenging while that in Fig. 15 represents a parameter named the scavenging collection efficiency.

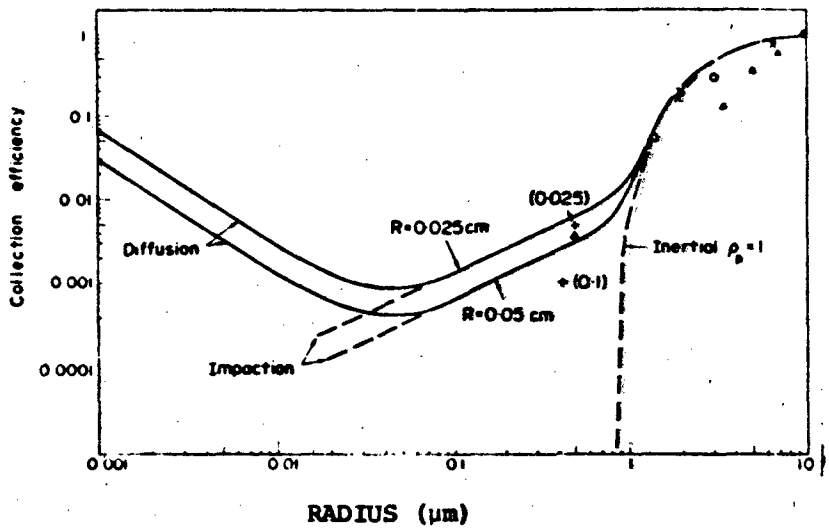

Fig. 15. Theoretical collection efficiencies (assuming complete retention) used in calculations, and selected experimental results. R refers to the raindrop size. Experimental: x. Starr and Mason (R - 0.05 cm)(1966): O. Walton and Woodcock (R - 0.05 cm)(1970): +. Adam and Semonin (R in ())(1970): Δ. Sood and Jackson (R - 0.05 cm)(1970): ▲. Engelmann (R - 0.02 cm)(1965). The abscissa is aerosol particle radius. (Adapted from Dana and Hales, 1976). Sources of experimental data are identified in the source paper.

Table 6. Conditions under which aerosol precipitation scavenging measurements were obtained (Radke et al., 1980).

Date	Source of scavenged aerosol particles	Location	Nature of cloud and precipitation scavengers	Scavenging time (s)	Average rain rate (mm h^{-1})
13 May 1974	Kraft-process paper mill	Port Townsend, Washington	Cumulonimbus with low cloud base; rain shower.	960	7
25 March 1976	Natural	Near Centralia, Washington	Cumulonimbus with medium cloud base; rain shower.	480	18
10 May 1976	Coal-fired power plant	Near Centralia, Washington	Stratocumulus precipitation with an orographic component; rain.	(a) 400 (b) 265	10
1 July 1976	Natural	Near Miles City, Montana	Cumulonimbus cluster, high cloud base, lightning discharges; heavy rain showers.	(a) 1800 (measurements taken at 3 km MSL) (b) 1100 (measurements taken at 2.5 km, MSL)	9
21 April 1977	Emissions from a volcanic maar	Near King Salmon, Alaska	Cumulonimbus with low cloud base; graupel shower.	300	12
29 June 1977	Coal-fired power plant (2100 MW)	Near Farmington, New Mexico	Isolated cumulonimbus with high cloud base; short period of light rain showers.	600	8

These parameters are not the same; we refer the reader to the source papers for a definition of the distinction. Both are indicators of washout efficiency, however.

The following features in Fig. 16, 17 and 18 are noted.

(1) A pronounced minimum in washout efficiency appears in every case. This minimum appears in the range of aerosol sizes from 0.4 to 1.1 μm diameter. Compare this to the theoretical minimum in Fig. 15 at 0.05 μm radius.

(2) Scavenging efficiency is high in every case for large particles. Effectively, it reaches 80 percent at 2-4 μm particle diameter and 100 percent for particles larger than 10-12 μm. This result agrees well with theoretical results shown in Fig. 15.

(3) The percentage of aerosol particles removed increases with increased scavenging time (May 10, 1976) for large particles and decreases for small particles. There is also a pronounced shift in the scavenging gap toward small aerosols with increased scavenging time.

(4) Measured scavenging efficiences for small particles are much greater than predicted from theory as shown in Fig. 15. This is believed to result, at least in part, from the fact that many of the small particles act as cloud condensation nuclei and appear in the experimental data as scavenged particles. Theory of Fig. 15 does not include this effect. This phenomenon may also partially explain the shift in the theoretical size for the scavenging gap toward larger particles in the experimental data. Nonetheless, the efficiencies for small particles are still substantially less than those of large particles.

(5) The pronounced increase in scavenging efficiency for large particles begins at about 1 μm to 10 μm in both theoretical and experimental data.

Theory and experiment show that washout and/or rainout are very important in removal of aerosol particles, particularly the large particles. For a maritime aerosol with high particle number counts above 2 μm, we can expect that the net effect of precipitation on the size distribution is to transform a typical maritime size distribution into a distribution more characteristic of continental aerosols.

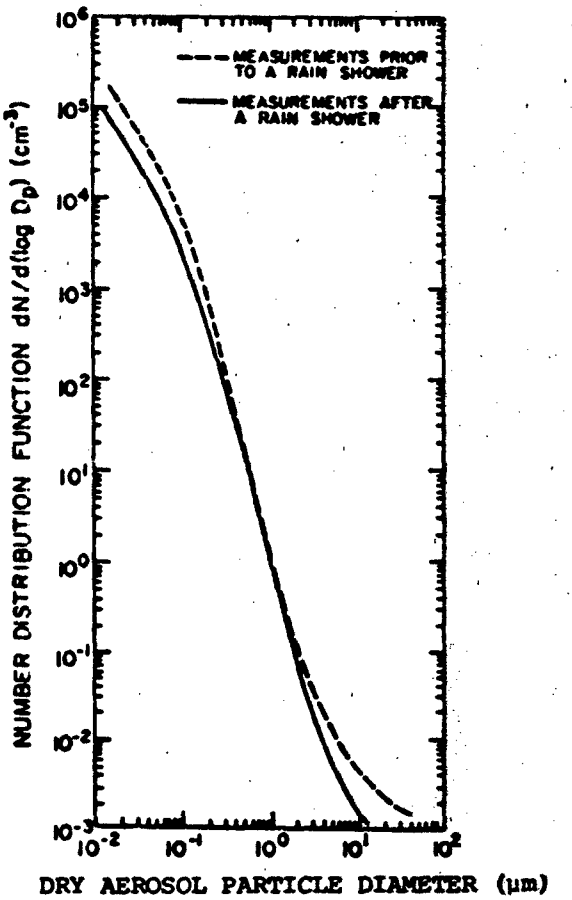

Fig. 16. Airborne measurements of the size spectra of aerosol in the plume from the coal-fired electric power plant near Centralia, Washington, measured at 5 km (12 min travel time) downwind of the stack on 10 May 1976, before and after the plume was intercepted by a rain shower (Radke et al., 1980).

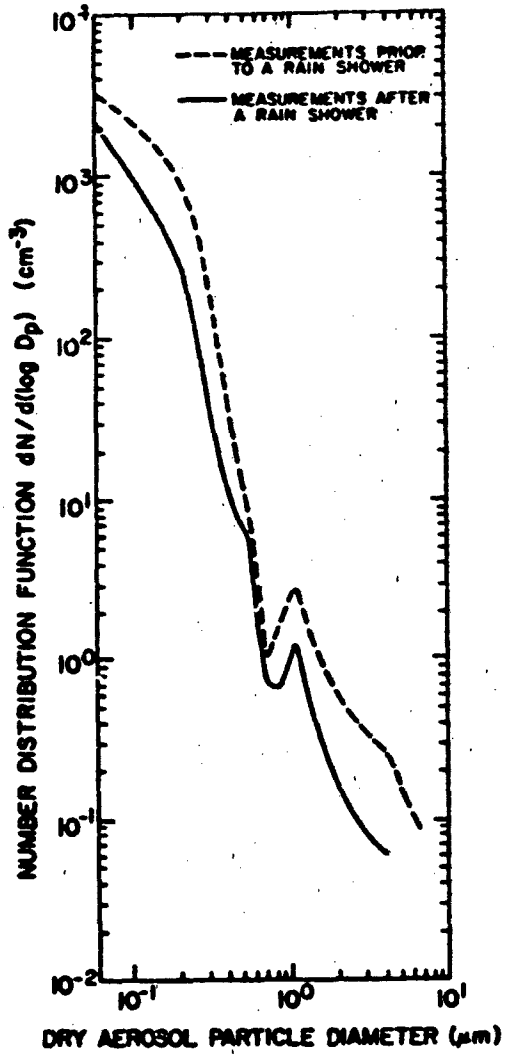

Fig. 17. As in Fig. 16 except for "natural" aerosol particles measured at an altitude of 2.5 km MSL near Miles City, Montana on 1 July 1976 (Radke et al., 1980).

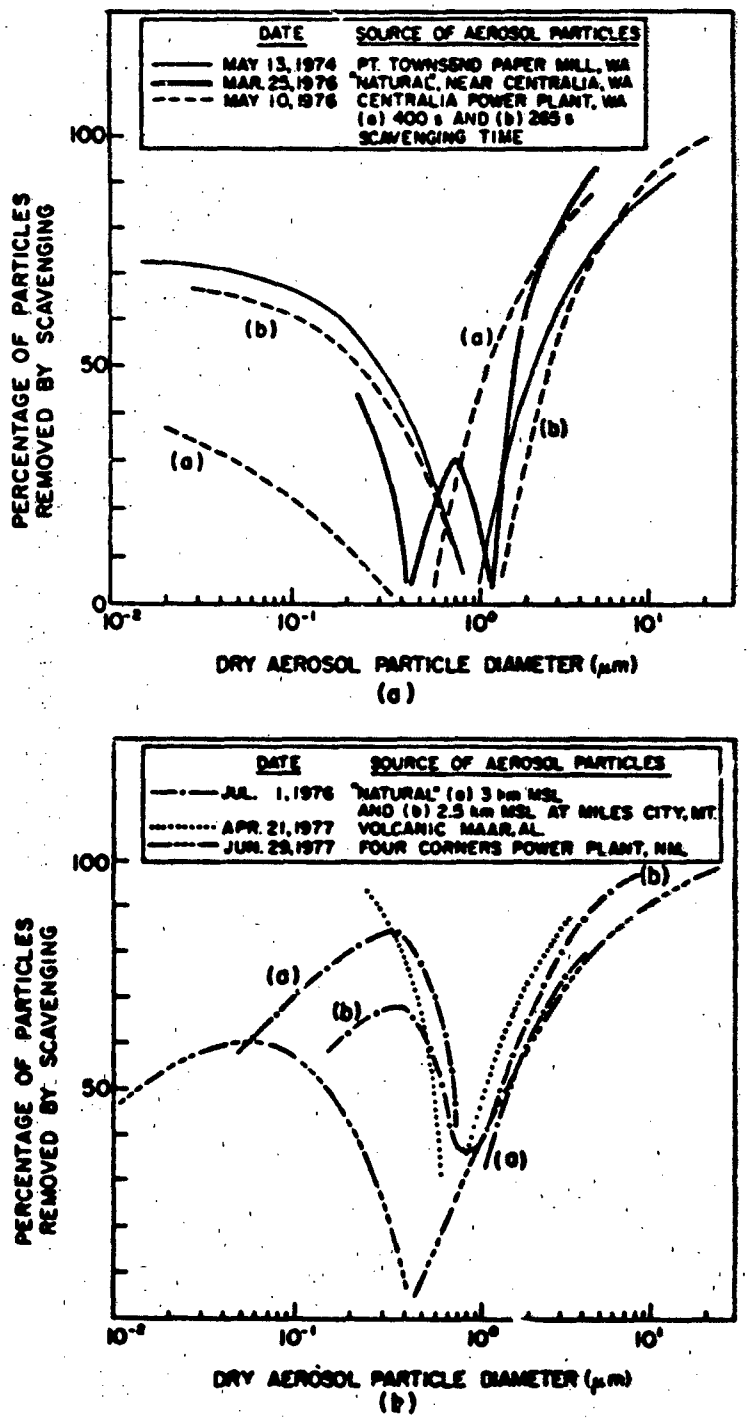

Fig. 18. Percentages of aerosol particles of various sizes removed by precipitation scavenging. See Table 6 for details on conditions under which measurements were obtained (Radke et al., 1980).

Processes Affecting the Urban Aerosol

Dispersion and pollutant source strengths are important in the TDA forecasting problem in assessing the concentration of urban aerosols. Table 7 contains data from selected sources on typical concentrations of Total Suspended Particles (TSP) as well as concentrations of the principal constituents in urban aerosols. A few reports also contain data on the fraction of the urban aerosol mass contained in the coarse particle range. The size limit boundary between the fine and coarse fractions is usually set at either 2.5 μm or 3.5 μm in studies of urban aerosols because this range represents the upper size limit of respirable particles. The following features in Table 7 are important for our purpose:

(1) Total Suspended Particulates (TSP) (interpreted as total mass concentration) have values typically 10-20 times those found in the natural aerosol.

(2) Carbon compounds are an important part of the urban aerosol. The majority are organic compounds. Some are soluble; some are not. The elemental carbon (EC) component (often referred to as soot) is almost entirely insoluble.

(3) Coarse particles often comprise a significant part of the total urban aerosol. This component is typically 20-60 percent of the total mass. The coarse particles are made up primarily of crustal materials (fly ash and soil derived aerosols). These materials are almost entirely insoluble.

(4) We found little data on the rate at which urban aerosols decrease in concentration beyond the urban area boundary. Junge (1963) reports that concentrations approach natural levels as near as 5 km from the boundary. Other sources have indicated similar ranges.

(5) The soluble sulfate and nitrate compounds are found almost entirely in the fine fraction. Their behavior is similar to that of the background aerosol; the variations in total concentration are often reflected in variations in particle mass in that component.

In the problem of LOWTRAN aerosol model selection, we based the

Table 7. Characteristic properties of various types of urban aerosols from selected sources. Junge (1963) reports a comparison to the natural aerosol. EC is elemental carbon. The boundary between fine and coarse fractions as reported by Wolff and Countess is about 3 μm.

Source	Location	Typical Concentrations ($\mu g\ m^{-3}$)					Percent Mass		Remarks
		SO_4^-	NO_3^-	Carbon		TSP	Fine	Coarse	
				Organic	Soot/EC				
Junge (1963)	Large Cities	22-25	6-20	40-60	. . . .	200-800			Pollution approaches background level within 5 km of city.
	Small Cities	4	3	25	. . . .	100-200			
	Natural Aerosol	. .	. . .	. . .	. . . .	5-50			
Wolff (1981)	Remote Areas	. .	. . .	. . .	0.2-1.1	. . . .	75	25	EC = 3-11 percent of TSP.
	New York	. .	. . .	. . .	4.2-13.3				EC ranges from 14 percent to 56 percent of total carbon.
	Portland	. .	. . .	. . .	10				
	Wash., D.C. . .	. .	. . .	. . .	6.5				
	Los Angeles . .	. .	. . .	. . .	3.1-4.0				Denver geometric mass median diameter for EC = 0.28 μm.
	Denver	. .	. . .	. . .	5.4	. . . .	82	18	
									Median diameter is typically 0.1 - 0.2 μm.
Countess et al. (1980)	Denver Winter								
	Range	0.2-67.9	0.0-59.7	1.5-31.2	0.2-30.9	45-200			76 percent of Coarse is Crustal (fly ash, Si, dust).
	Average	3.9	5.0	9.2	6.6	. . . .	23	77	
	Percent Fine	77	82	71	82				10 percent of Coarse is EC

selection criteria for the urban model on the assessment of the expected concentrations of the urban aerosol. This concentration at a given time will depend on the strength of the urban aerosol sources and on those meteorological conditions which control the effectiveness of dispersion mechanisms. Appendix A describes how we arrived at selection criteria based on a classification of the total source strength of an urban area and on boundary layer wind speed and stability conditions.

5 FACTORS THAT DETERMINE EXTINCTION EFFICIENCY

Aerosol scattering at a particular wavelength is commonly expressed in terms of the scattering efficiency, Q_S. The equation

$$1 - T_S = Q_S \pi r^2$$

states the relationship for a single particle of radius, r, in a unit volume. T_S is transmission; $(1 - T_S)$ represents the fractional depletion, per unit of distance through the volume, of the incident energy by the particle.

The scattering efficiency is related to the scattering cross-section, σ_S, by

$$\sigma_S = Q_S \pi r^2$$

The scattering cross-section expresses the effectively scattering cross-sectional area in relation to the physical cross-sectional area. The scattering efficiency defines the relationship.

The corollary parameter, Q_E, the extinction efficiency, defines this relationship for the combined effects of scattering and absorption. The extinction efficiency is dependent, from Mie theory, on two parameters, the complex refractive index, and the ratio of particle size to wavelength (r/λ) where λ is the wavelength of incident radiation.

The complex refractive index is commonly expressed in the form

$$m = n + in',$$

where n and n' are the real and imaginary parts respectively. The real part represents scattering while the imaginary part represents absorption. Volz (1972) has reported refractive index data for a variety of aerosol substances. Both parts show considerable variability in their values among the different substances. In general, the real part of the refractive index becomes quite variable in the middle infrared region and increases slightly in the far infrared region. The imaginary part increases markedly with increasing wavelength, particularly for the water

soluble continental aerosols. Many aerosol substances have absorption indices in the range 0.1 to 0.3 at 8-12 μm. Strongly absorbing carbon compounds have indices about 0.5. Even for strongly absorbing aerosols, however, the effect of refractive index variations on extinction efficiency is small compared to the effect of particle size.

The extinction efficiency of aerosol particles at a specified wavelength depends very strongly on particle size. This dependence is usually expressed in terms of the generalized size parameter α_ε, after Hänel (1976),

$$\alpha_\varepsilon = \frac{2\pi r}{\lambda} \{(n-1)^2 + n'^2\}^{\frac{1}{2}}$$

Fig. 19 shows the extinction efficiency versus the generalized size parameter for several refractive index values. The value of the size parameter is primarily dependent on the ratio r/λ; we see that the extinction efficiency is very low for particles with size parameter less than 2. Table 8 shows the values of σ_ε for several particle sizes and refractive index values. The table contains values of extinction efficiency taken from Fig. 19. The data show that visible (.55 μm) extinction efficiency is relatively uniform in the size range indicated. Extinction efficiency at 10 μm, on the other hand, is very low for small particles. Only weak far infrared extinction occurs for particles smaller than 2 μm, even for those with a strong absorption component as represented by the third value of the refractive index in Table 8. This result implies that when high concentrations of the small particles are present, even in concentrations that may result in rather low visibility values, the 8-12 μm transmission by aerosols may remain high.

The preceding discussion suggests that aerosol extinction in the 8-12 μm band depends primarily on the presence of particles larger than about 2 μm. The case studies presented in Section 3 show that significant numbers of particles in this size range can be expected in the natural aerosol only in the marine aerosol or when windblown dust particles are present. These large particles may also result from man-made sources and exist in the form of dust or fly ash.

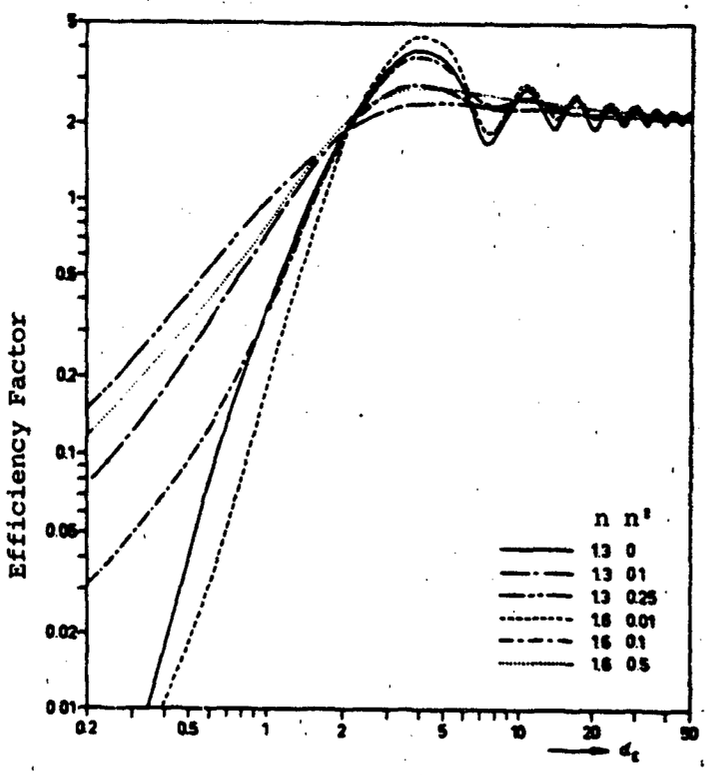

Fig. 19. Efficiency factor of extinction versus generalized size parameter α_E as computed from Mie theory for several complex refractive indices n - in'. (Adapted from Hänel, 1976).

The extinction efficiency at 1.06 μm is lower for particles smaller than 1 μm than for the corresponding efficiencies at 0.55 μm. The efficiencies are much higher, on the other hand, than those at 10 μm for the same particles. Particles 1 μm or greater attenuate very efficiently at 1.06 μm. Following the argument above, these data show that attenuation at 1.06 μm is significant whenever particles larger than 0.2 μm are present in significant concentrations. This condition is in marked contrast to the requirement for particles larger than 2 μm for significant extinction in the 8-12 μm band.

Table 8. Size parameters (α_E) and extinction efficiency values (Q_E) as a function of refractive index (m) and particle radius at three radiation wavelengths. The extinction efficiencies were taken from Fig. 19.

λ (μm)	Radius (μm)	m = 1.3 + 0.0i		m = 1.3 + 0.1i		m = 1.6 + 0.5i	
		α_E	Q_E	α_e	Q_E	α_E	Q_E
0.55	.2	.685	.07	.723	.4	1.78	1.4
	.5	1.71	1.3	1.80	1.3	4.45	2.6
	1.0	3.43	2.3	3.61	2.1	8.92	2.3
	2.0	6.85	2.4	7.22	2.0	17.8	2.2
	5.0	17.1	2.2	18.1	2.0	44.6	2.0
	10.0	34.3	1.1	36.1	2.0	89.2	2.0
10	.2	.0377	∿0	.0397	∿0	.0981	∿0
	.5	.094	∿0	.099	∿0	.245	.16
	1.0	.188	∿0	.199	.08	.491	.3
	2.0	.377	.015	.397	.18	.981	.7
	5.0	.943	.3	.994	.7	2.45	2.1
	10.0	1.88	1.1	1.99	1.7	4.91	2.3
1.06	.2	.355	.03	.375	.27	.941	.85
	.5	.887	.28	.937	.65	2.35	2.1
	1.0	1.78	2.0	1.87	2.0	4.63	2.7
	2.0	3.56	3.6	3.75	3.5	9.23	2.5
	5.0	8.87	2.5	9.39	2.5	23.1	2.2
	10.0	17.8	2.3	18.7	2.3	46.3	2.1

6 RELATIVE HUMIDITY EFFECTS

Soluble aerosol particles absorb liquid water on their surfaces and grow in size when relative humidity increases. For highly soluble compounds when the relative humidity reaches a critical value, the particles go into liquid solution and a step increase in particle size occurs. The critical relative humidity for pure sodium chloride is about 76 percent; the value for pure ammonium sulphate is about 81 percent.

Particle growth with increasing relative humidity acts in two ways to change the aerosol extinction properties. The principal effect is through the change in the size distribution. The absorption of water effectively shifts the entire distribution of the soluble particles to larger sizes. This increase in size enhances the extinction efficiency of the particles at longer wavelengths. The aggregate effect is significantly greater extinction at those wavelengths. A secondary but important effect of increasing relative humidity is the change in the refractive index of the particles. As the particle water content increases, the refractive index of the particle approaches that of water.

This section emphasizes two important ideas regarding relative humidity effects. The first is that the growth behavior of the soluble particle depends on its specific chemical composition. The second idea illustrates the effect of relative humidity increases in the LOWTRAN modeled number density and surface area distributions, compares these distributions between the rural and maritime models, and discusses implications for infrared extinction.

Much of the current understanding of relative humidity effects derives from extensive theoretical and experimental work by Hänel. His early work is published in Volume 19 of Advances in Geophysics (Hänel, 1976). This reference details the theoretical foundation for prediction of particle growth with changing relative humidity.

Hänel and Lehmann (1981) report recent experimental data on the dependence of growth on chemical composition of the aerosol. Figure 20 presents a comparison of the size dependence on relative humidity for two different aerosol types. The curves were derived from the observed

chemical composition of the two aerosols and their predicted growth behavior. The Mace Head, Ireland aerosol was a marine aerosol with a large sea-salt mass component. The growth curve shown is for the sea-salt particles. The Hohenpeissenberg, Germany aerosol was a continental aerosol composed almost entirely of ammonium sulphate, ammonium nitrate and sulfuric acid.

The curves in Figure 20 show that the equilibrium size of a particle during changing relative humidity depends on the direction of the relative humidity change. This hysteresis effect is due primarily to the existence of super-saturated solutions in the droplet during periods of decreasing relative humidity. The practical importance of the hysteresis effect to the TDA forecasting problem is small and occurs over a narrow relative humidity range. The LOWTRAN aerosol models do not account for this effect. Their tendency within this range is to overestimate extinction slightly during increasing relative humidity and to underestimate during decreasing relative humidity.

The primary feature of Fig. 20 is the difference in growth behaviors of the two aerosol compounds. The sea-salt compounds show a much stronger relative humidity response than the compounds in the continental aerosol.

The effect of aerosol response to relative humidity changes is modeled in LOWTRAN by changing the size distributions. Fig. 21 shows the number density distributions of the rural and maritime models at four different values of relative humidity. The total particle number concentration is fixed at 15000cm^{-3} in the rural model and at 4000cm^{-3} in the maritime model. In the maritime distribution one percent of the particles are of a marine origin.

Table 9 shows approximate values of the number densities for a range of particle sizes for the rural and maritime models. Number densities are given at zero and 99 percent relative humidity in each model. The third column under each model shows the approximate ratio of number density at 99 percent to that at zero percent.

Note the following features:

(1) At zero percent relative humidity, the maritime model

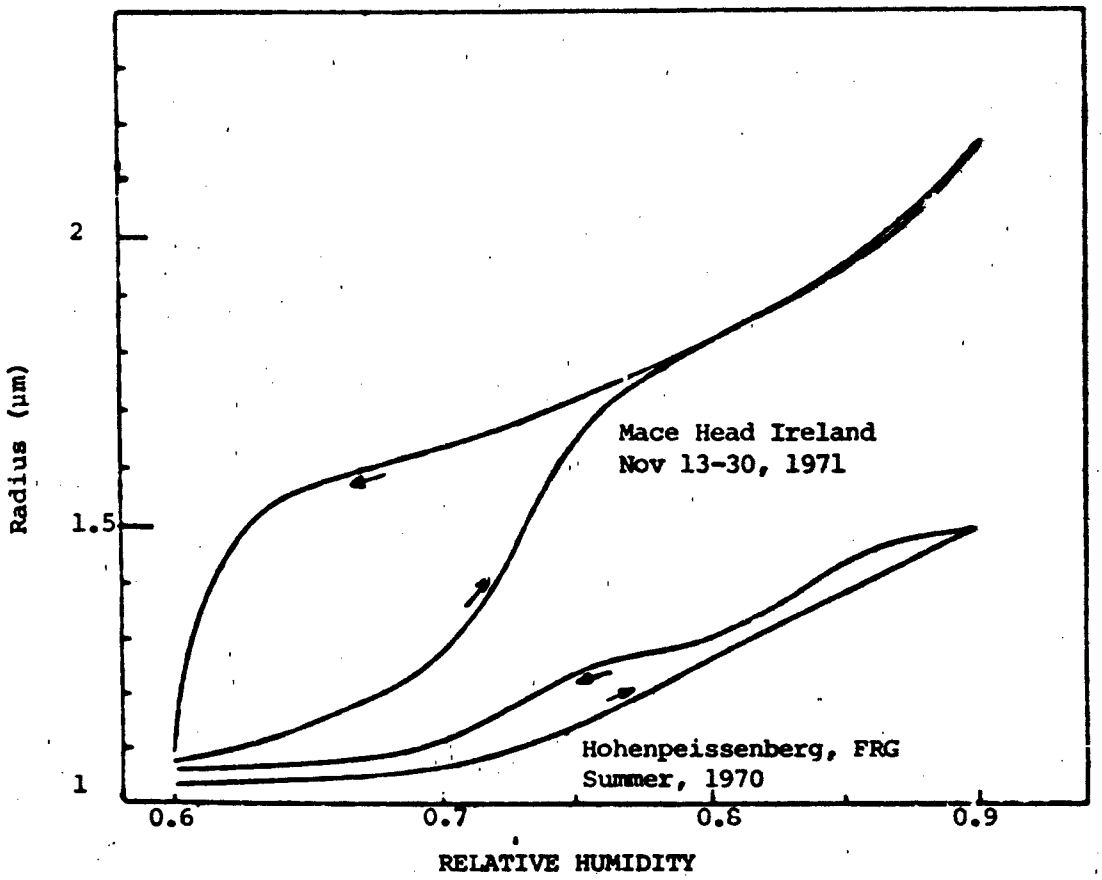

Fig. 20. Hysteresis curves for maritime aerosols (Mace Head, Ireland) and continental aerosols (Hohenpeissenberg, Germany). Arrows indicate the direction of the humidity change represented by each curve. (Adapted from Hänel and Lehmann, 1981).

contains significantly higher concentrations than the rural model in the size range 0.8 μm to 2.0 μm. The mode radius for the sea-salt particles at zero percent relative humidity is approximately 0.2 μm. The differences in the number concentrations in the range from 0.8 μm to 2.0 μm are due to the large particle tail of the sea-salt mode distribution.

(2) The number densities in the size range above the 2 μm increase at 99 percent relative humidity in much higher ratio in the maritime model than in the rural model. This reflects the strong growth response of the sea-salt aerosol compared to that of the continental aerosols. The mode radius of the sea-salt aerosol at 99 percent relative humidity is about 0.75 μm; those of the two modes in the continental aerosol are about 0.05 μm and 1.17 μm respectively. However, the number

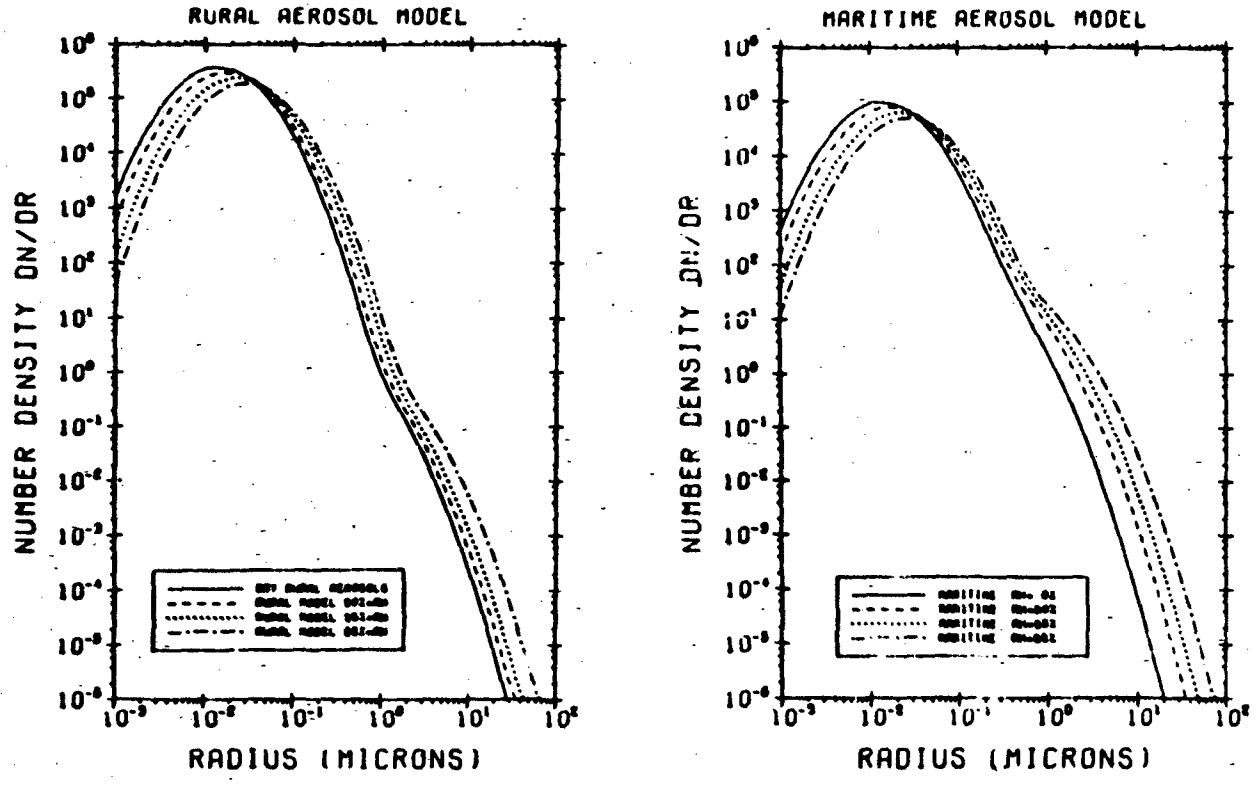

Fig. 21. A comparison of number density distributions in the LOWTRAN rural and maritime models at four values of relative humidity (Shettle and Fenn, 1979).

Table 9. Approximate number densities of particles of various sizes at relative humidities of zero percent and 99 percent in the rural and maritime models. The third column under each model shows the approximate ratio (R) of the number density at 99 percent relative humidity to that at zero percent.

Radius (μm)	Number Densities (μm^{-1})					
	Rural			Maritime		
	0	99	R	0	99	R
.2	1.7×10^{3}	9.7×10^{3}	5:1	6×10^{2}	3×10^{3}	5:1
.4	9×10^{1}	7.9×10^{2}	9:1	5×10^{1}	2.5×10^{2}	5:1
.6	1.0×10^{1}	1.0×10^{2}	10:1	1.3×10^{1}	6×10^{1}	5:1
.8	2.5×10^{0}	4.0×10^{1}	16:1	6×10^{0}	3×10^{1}	5:1
1.0	8.0×10^{-1}	8×10^{0}	10:1	2.5×10^{0}	2×10^{1}	8:1
2.0	1.2×10^{-1}	6.0×10^{-1}	5:1	2×10^{0}	6×10^{0}	30:1
4.0	1.4×10^{-2}	9.0×10^{-2}	6:1	9×10^{-3}	8×10^{-1}	88:1
6.0	2.5×10^{-3}	3×10^{-2}	12:1	1.2×10^{-3}	2×10^{-1}	166:1
8.0	8×10^{-4}	1.2×10^{-2}	15:1	2.5×10^{-4}	9.5×10^{-2}	380:1
10.0	3×10^{-4}	6×10^{-3}	20:1	6×10^{-5}	3×10^{-2}	500:1

concentration in the second continental mode is much less than the marine aerosol counts in the maritime model.

(3) The ratio of number densities in the size range below 0.8 μm is somewhat higher in the rural model than in the maritime model. This difference reflects the dominance of the rural model size distribution by the continental aerosol. The increase in the number densities for the particles below 0.8 μm represents growth of the soluble continental aerosols.

Referring back to Figures 1 and 2 in Section 1, we may explain the differences in the extinction properties modeled in the rural and maritime models as follows:

In the 8-12 μm band, the strength of the aerosol extinction depends mostly on the presence of the sea-salt aerosol. In section 5, we showed that significant extinction in this spectral region required the presence of particles larger than 2 μm. Table 9 shows that these particles are modeled in great numbers only in the maritime model at high relative humidities.

The relatively high numbers of the large particles combined with their high extinction efficiency at this wavelength produce the observed behavior of the maritime model's 8-12 μm transmission shown in Fig. 1.

At 1.06 μm, we observed a significant difference in Fig. 2 in the maritime model transmission compared to that of the rural model for a given visibility. The relative humidity response of each of the models was small. We showed, in Section 5, that 1.06 μm extinction is dependent on the number density of particles larger than 0.2 μm. Table 9 shows that these particles are always present in both models in significant numbers. Hence, the 1.06 μm extinction is much greater in either model than that at 8-12 μm.

The differences between the maritime and rural model extinctions at 1.06 μm at a given visibility are explained by the presence or absence of the sea-salt aerosol. The size range of the sea-salt particles across the relative humidity range from zero to 100 percent is such that they are effective attenuators of 1.06 μm radiation at all relative humidities. Their presence in the maritime model simply increases the relative concentration of effective 1.06 μm attenuators at all relative humidities.

The difference in the extinction properties of the urban model compared to the rural model is of less importance than the differences due to the marine aerosol. The observed differeces between the rural and urban models are due to the soot-like aerosols in the urban model. Since these particles are insoluble, their effect is to make the urban model less responsive to relative humidity changes than the rural model.

7 THE AEROSOL MODEL SELECTION ALGORITHM

The Aerosol Model Selection Algorithm assumes that the most important consideration in selection is the presence or absence of the sea-salt aerosol. When sea salt is thought to be present in sufficient concentrations, then the maritime model takes precedence over the rural and urban models for predicting infrared extinction, even if urban pollution is present. If sea salt is not thought to be present in sufficient concentrations, then the rural model is recommended for the boundary layer except when urban pollutants are present; in that case, the algorithm provides criteria for selection of the urban model over the rural model.

The criteria for determining whether sea-salt aerosols are present are based on three considerations: (1) the origin of the airmass, (2) possible addition of sea-salt aerosols during airmass travel, and (3) evaluation of mechanisms for removal of the sea-salt aerosol after landfall of the airmass.

The role of airmass type in defining the presence of sea salt is evident in data published by Duncan and Lindberg (1981). They fit observed particle size distributions in Europe to a bimodal distribution model and performed Mie scattering calculations at 0.55 μm and 10 μm. Fig. 22, taken from their report, presents a plot of extinction coefficients at 10 μm versus extinction coefficients at 0.55 μm. The size distributions were measured in German weather conditions during three periods: February-March 1978, November 1978, and February-March 1980. Visibility conditions varied from light haze to dense fog. The data represent measurements in three airmass types: continental polar, maritime arctic, and maritime polar. Note the wide scatter of the data plots and the apparent separation by airmass type.

Figs. 23, 24 and 25 are plots of the same data set after the data were separated according to airmass type. The data scatter is much reduced in comparison with Fig. 22. An overlay of these plots would show some differences between continental polar air and the two types of maritime air.

The algorithm assumes addition of the sea-salt aerosol when continental airmasses travel over open ocean enroute to the point of interest.

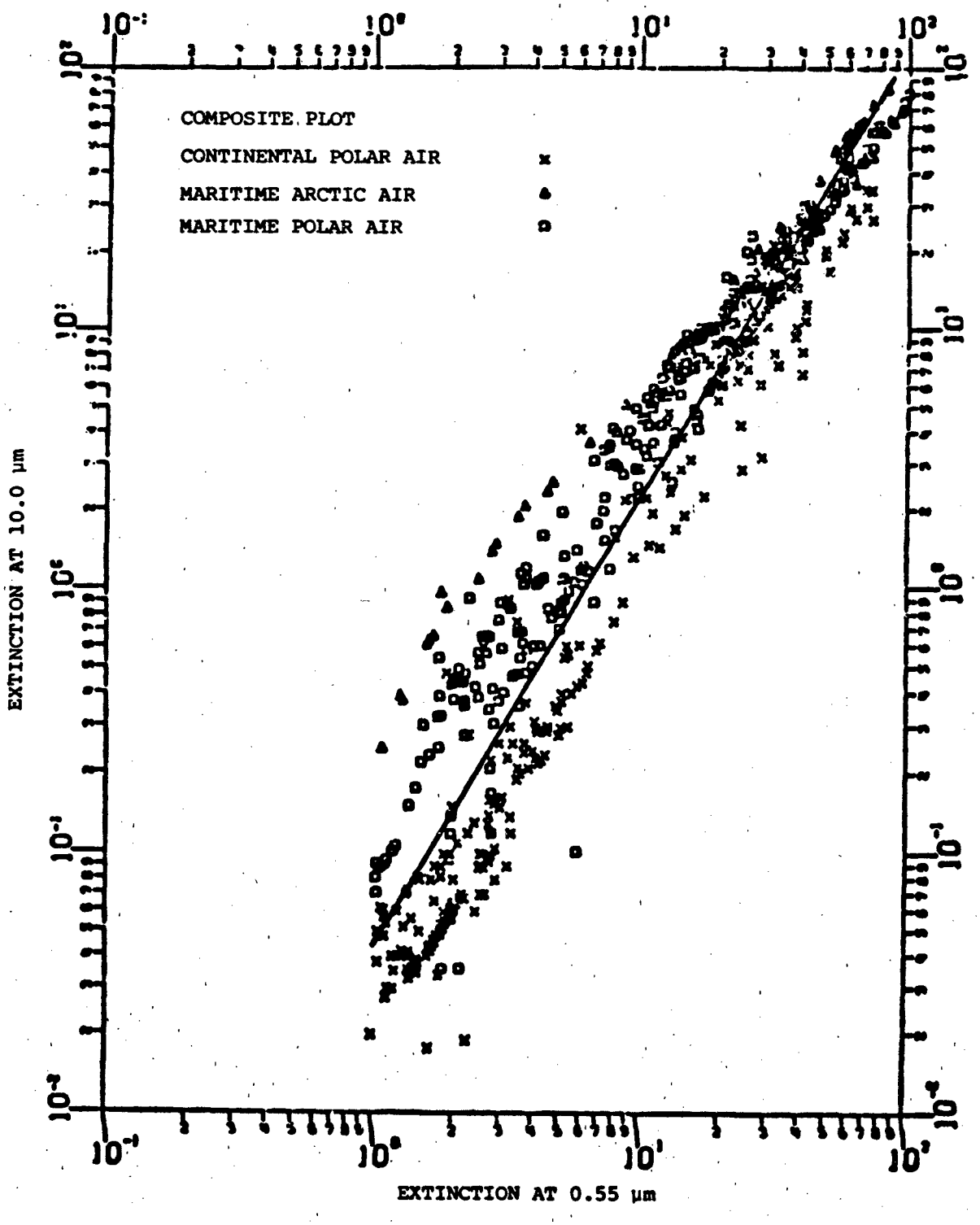

Fig. 22. Composite plot of extinction coefficient at 10 μm versus extinction coefficient at 0.55 μm (units are km^{-1}) (Duncan and Lindberg, 1981).

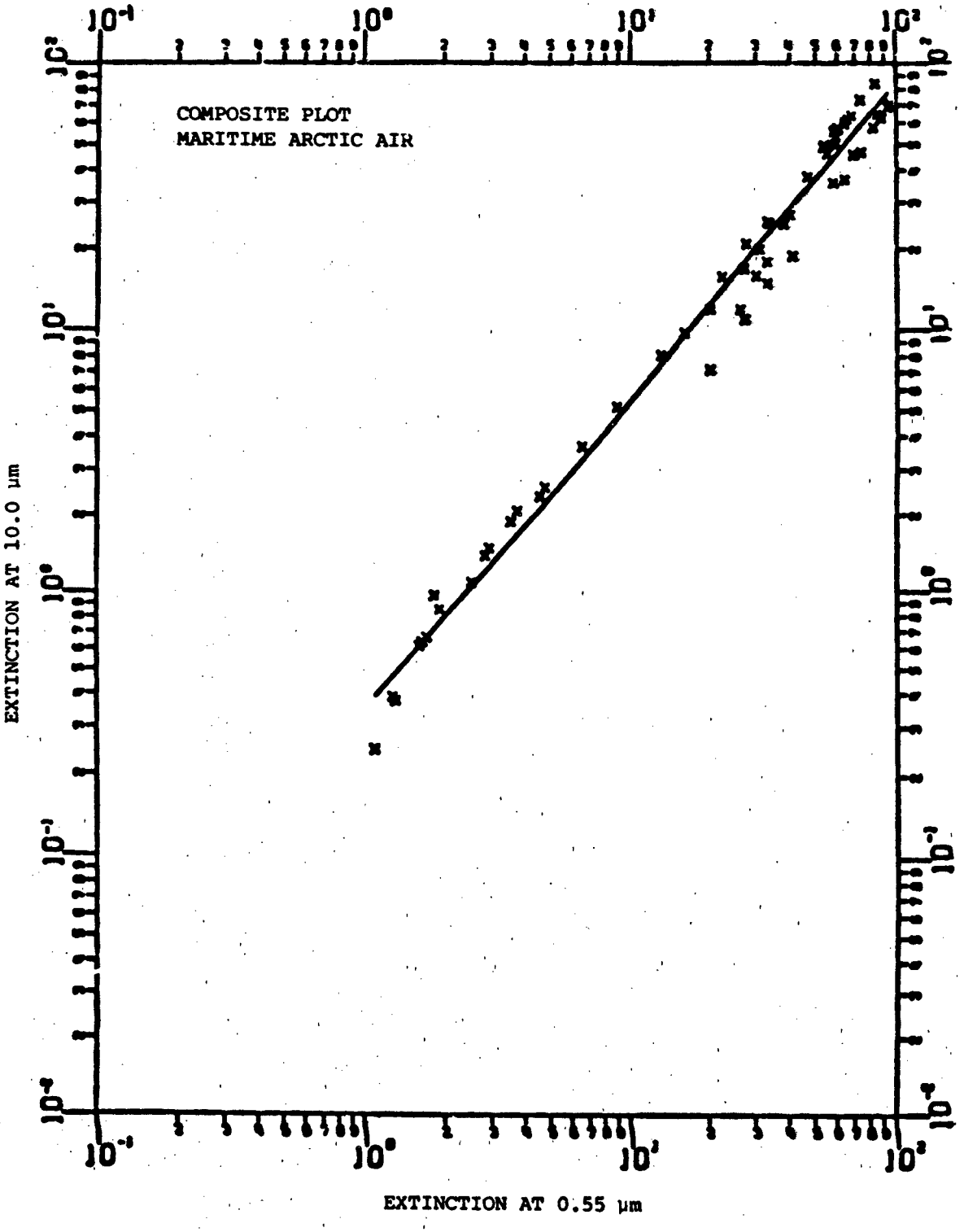

Fig. 23. The portion of the data shown in Fig. 22 where the site was under a maritime arctic airmass (units are km^{-1}) (Duncan and Lindberg, 1981).

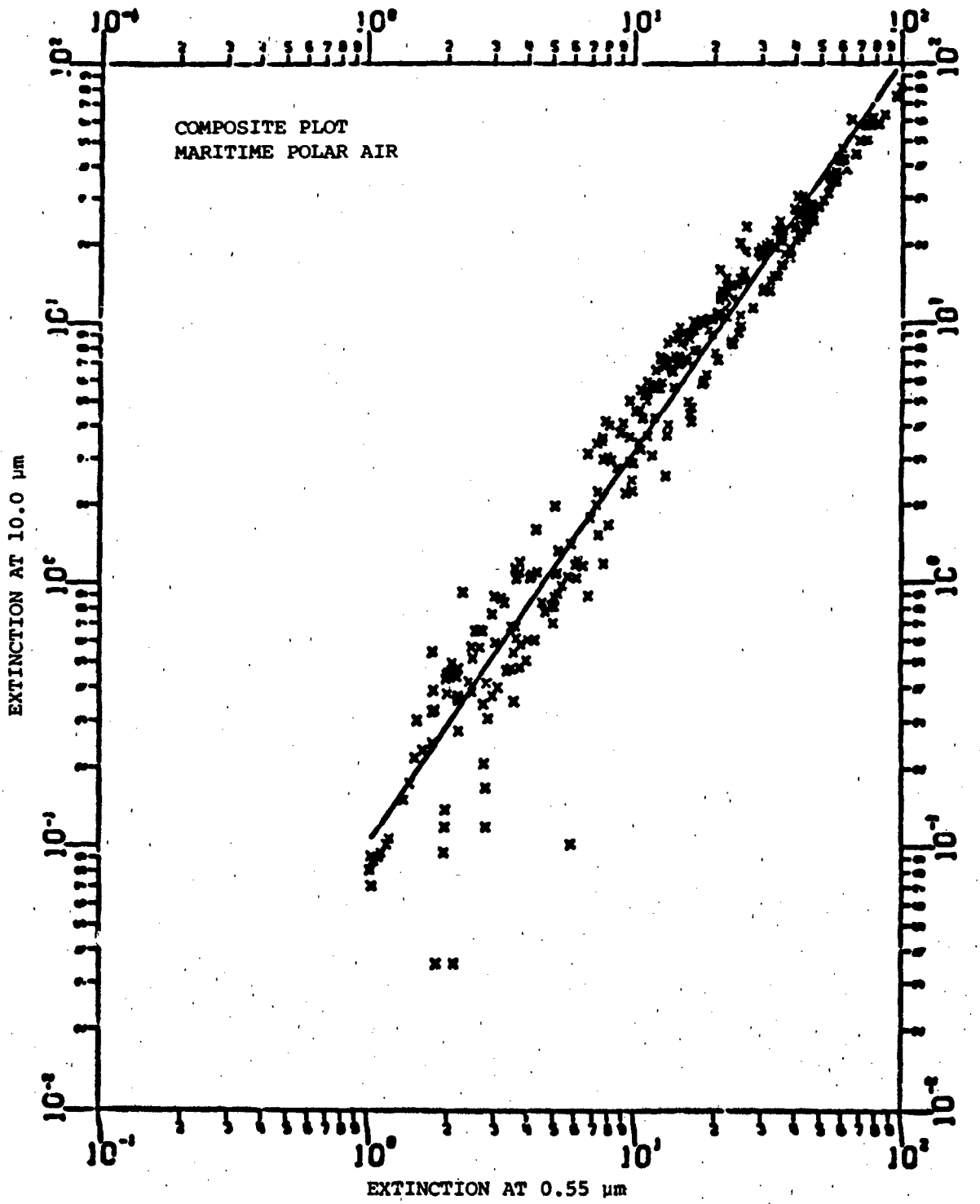

Fig. 24. Same as Fig. 23 except for maritime polar airmass (Duncan and Lindberg, 1981).

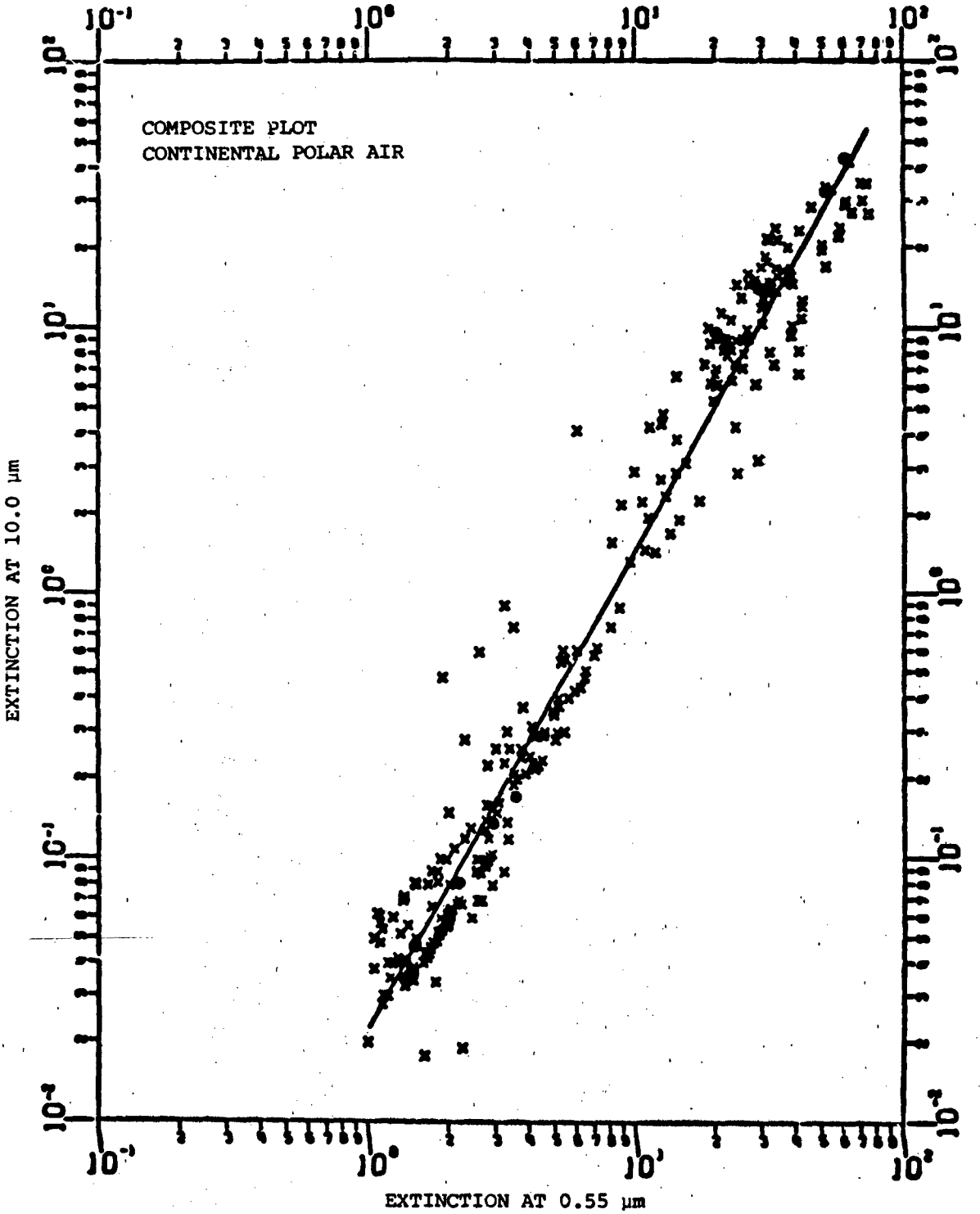

Fig. 25. Same as Fig. 23 except for continental polar airmass (Duncan and Lindberg, 1981).

The length of oceanic trajectory required for use of the maritime model is assumed to be longer for airmasses traveling over cold water than for those traveling over warm water. The specific values of 800 km and 500 km for trajectory length are only estimates. This criterion is a means of accounting for the effect of static stability on the relative effectiveness of mechanisms for vertical transport of the sea-salt particles.

Two mechanisms for removal are considered. The algorithm assumes that most sea-salt particles larger then 2 μm will be lost by sedimentation within three days after landfall of the airmass. The algorithm also assumes that any precipitation of moderate or greater intensity will remove most of the sea-salt particles. If either of the above criteria is met, then the rural model is recommended, even for airmasses of maritime origin.

Urban model selection criteria are based on the strength of the urban pollution source, the effectiveness of ventilation by the boundary layer wind, and effect of static stability on vertical dispersion. Appendix A describes how the selection criteria were developed.

Fig. 26 presents the logic chart which constitutes the selection algorithm. The following briefly describes the organization of the chart.

(a) Fig. 26-A separates airmasses by origin, and treats the possible transformation of an airmass with a continental origin and an oceanic trajectory.

(b) Fig. 26-B treats the mechanisms for removal of the sea-salt aerosol from a maritime airmass, namely, sedimentation and washout.

(c) Figs. 26-C and 26-D treat the problem of determining when the urban model should be used to describe a polluted continental aerosol. The urban model logic arrives at a critical value of the forecast boundary wind speed. When the forecast wind speed is less than the critical value, use of the urban model is recommended.

Fig. 26-A

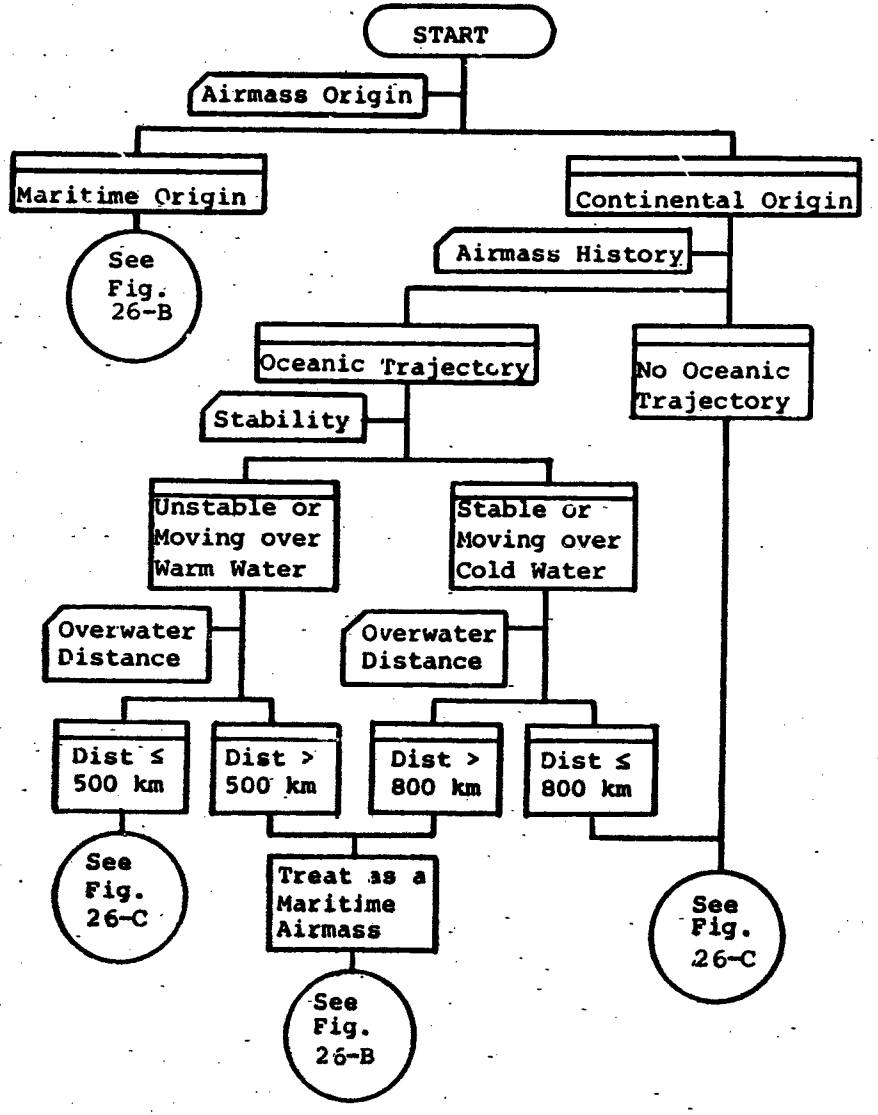

Fig. 26-B

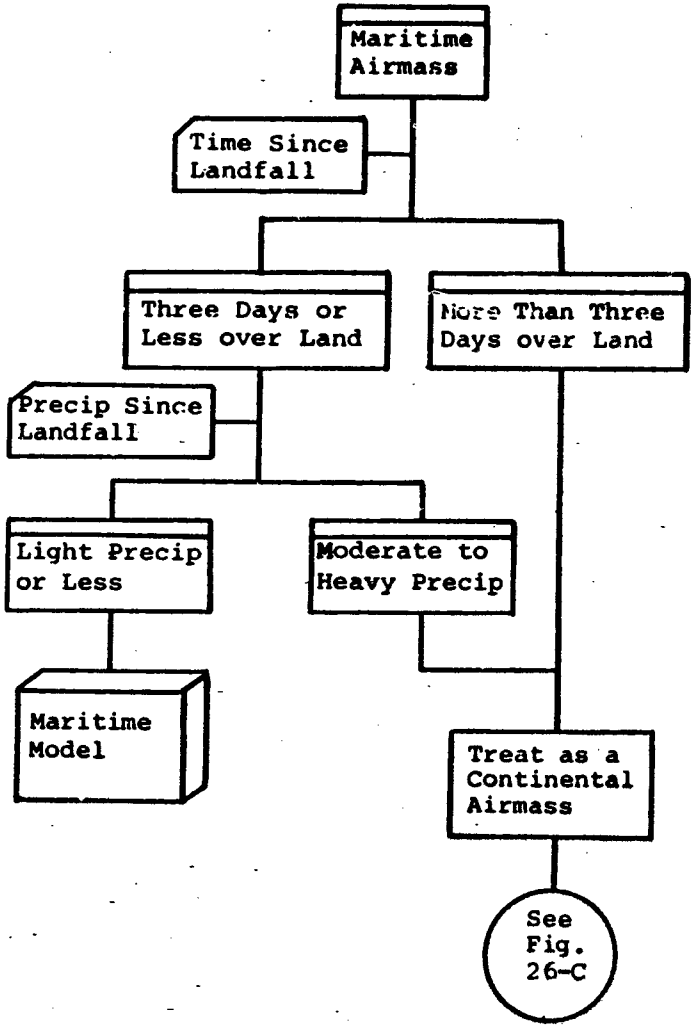

Fig. 26. The aerosol model selection process.

Fig. 26-C

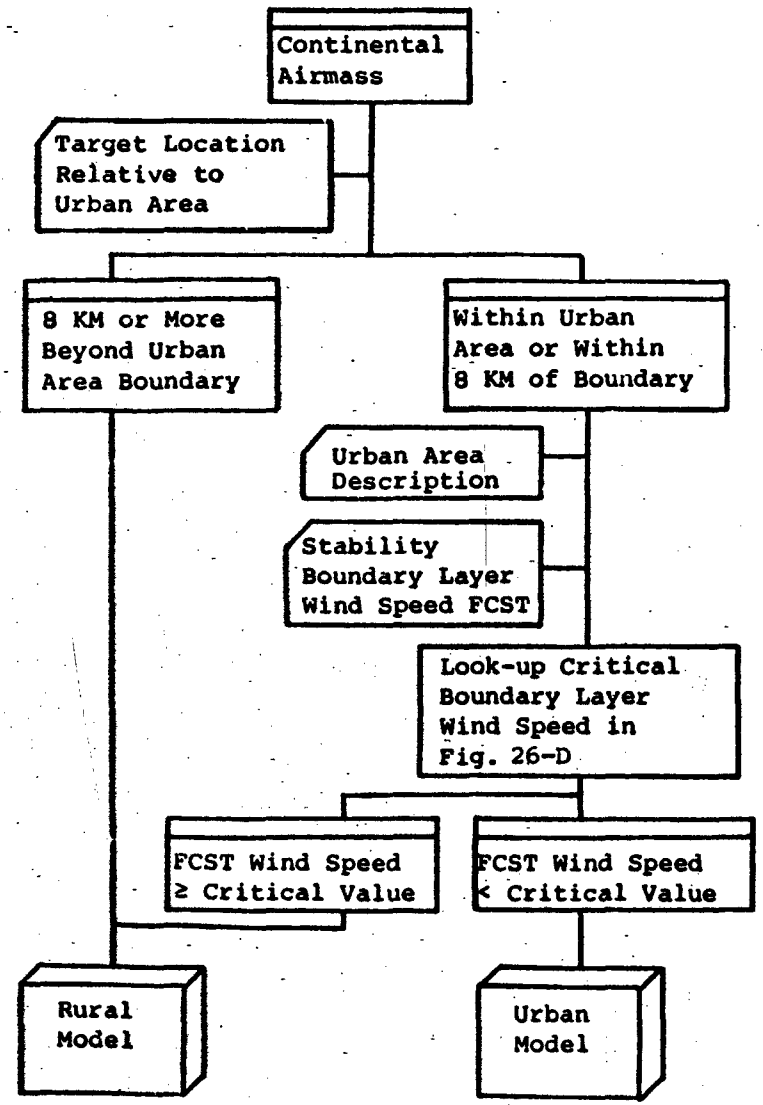

Fig. 26-D

Stability Condition	Critical Wind Speed (Knots)	
	Large and Heavily Industrialized Urban Areas (Area > 2000 KM^2)	Small - Medium Urban Areas or Large Areas Without Heavy Industrialization
Unstable	4	3
Neutral	8	5
Stable	25	15

Definitions of Stability:

1) Unstable: Lapse rate near dry adiabatic in lowest 1.5-2.0 KM enhances vertical diffusion.

2) Neutral: Lapse rate near the pseudo-adiabatic lapse rate or slightly more stable in the lowest 1.5-2.0 KM, with perhaps a weak inversion in the lowest 2 KM.

3) Stable: A strong inversion below 2 KM inhibits turbulent vertical diffusion.

Fig. 26-D. Approximate values of critical boundary layer wind speed (knots) for use of the urban aerosol model. Wind speed is tabulated against the size of the urban area and the stability condition. Definitions of stability categories are given above.

Fig. 26. (Continued)

8 SUMMARY AND CONCLUSION

Section 1 describes how the LOWTRAN aerosol models show the dependence of infrared extinction on the nature of the aerosol. Effective application of LOWTRAN in operational prediction of infrared extinction requires some means of estimating aerosol properties to aid in "best" aerosol model selection.

In Section 2 we described various methods of characterizing aerosols. The total number concentration and number density versus size distribution has a primary effect on the spectral dependence of extinction. Water solubility and specific chemical composition are the primary factors in determining the aerosol growth response to changes in relative humidity.

The descriptive case studies in Section 3 show the principle differences in various types of aerosols. The sudies showed the existence of the global background aerosol. This component of the aerosol shows little variability in space and time. The variable aerosol components are superimposed on the background aerosol and consist principally of three aerosols: sea salt, urban pollutants and windblown dust.

Section 4 describes the processes that determine the important time and space variability in aerosol properties. Continuous steady-state production mechanisms maintain the global background aerosol. Sea-salt aerosol production by the wind, aerosol production in urban and industrial complexes, and windblown dust are the most important sources of the variable components. The principle aerosol removal mechanisms on a large scale are sedimentation and rainout/washout. Dispersion is important in dilution of urban aerosol concentrations. We found that precipitation and washout are most effective in removal of the aerosols larger than 2 μm.

In Section 5 we showed the importance of the number density of various particle sizes in determining the wavelength dependence of extinction. Strong aerosol extinction at 8-12 μm requires significant concentrations of particles larger than 2 μm. Near IR extinction (e.g., 1.06 μm) depends primarily on the concentration of particles in the size range from 0.2 μm to 0.8 μm.

Section 6 emphasized two important points regarding aerosol

growth with increasing relative humidity. The growth behavior of soluble aerosols depends on their chemical composition; sea-salt aerosols exhibit a growth response much stronger than that of continental aerosols. The change in number density distribution with increasing relative humidity results in a strong relative humidity dependence of 8-12 μm extinction in marine aerosols.

Relative humidity dependence at 1.06 μm on the other hand is relatively weak. The maritime aerosols exhibit much stronger extinction than the continental aerosols. This difference is explained by the presence of sea salt, which is an effective attenuator at 1.06 μm across its entire range of particle sizes.

The general conclusion is that the primary contributor to variability in infrared extinction is the sea-salt aerosol. The first-order forecasting problem is to assess the presence of this component. Studies of known production and loss mechanisms and of the dependence of extinction properties on airmass type indicate that a reasonable assessment can be made from an analysis of airmass history. Airmass analysis is the primary basis of the Aerosol Model Selection Algorithm.

REFERENCES

Bigg, E. K., 1980: Comparison of aerosol at four baseline atmospheric monitoring stations. J. of Appl. Meteor., 19:521-533.

Countess, R. J., G. T. Wolff, and S. H. Cadle, 1980: The Denver winter aerosol: A comprehensive chemical characterization. J. of the Air Pollution Control Assoc., 30(11):1194-1200.

Dana, M. T. and J. M. Hales, 1976: Statistical aspects of the washout of polydisperse aerosols. Atmos. Environ., 10:45-50

Duncan, L. D., and J. D. Lindberg, 1981: Air Mass Considerations in Fog Optical Modeling. ASL-TR-0073, Atmospheric Sciences Laboratory, U.S. Army Electronics Research and Development Command, White Sands Missile Range, NM.

Eriksson, E., 1957: The chemical composition of Hawaiian rainfall. Tellus, 9:509-520

Gifford, F. A., and S. R. Hann, 1973: Technical note, modelling air pollution. Atmos. Env., 7:131-136

Hänel, G., 1976: The properties of atmospheric aerosol particles as functions of relative humidity at thermodynamic equilibrium with the surrounding moist air. Advances in Geophysics, Vol. 19, 1976, Academic Press:73-188.

Hänel, G., and M. Lehmann, 1981: Equilibrium size of aerosol particles and relative humidity: New experimental data from various aerosol types and their treatment for cloud physics application. Contributions to Atmospheric Physics, 54:57-71.

Hanna, S. R., 1978: Diurnal variation of the stability factor in the simple ATDL urban dispersion model. J. of the Air Poll. Control Assoc., 28:147-150

Junge, C. E., 1963: Air Chemistry and Radioactivity. International Geophysics Series, Vol 4. Academic Press, New York.

Junge, C. E., 1972: Our knowledge of the physico-chemistry of aerosols in the undisturbed marine environment. J. of Geophys. Res., 77 (27: 5183-5200.

REFERENCES
(Continued)

Junge, C. and R. Jaenicke, 1971: New results in background aerosol studies from the Atlantic expedition of the R. V. Meteor, Spring, 1969. J. of Aerosol Sci., 2:305-314.

Kasten, F., 1968: Falling speed of aerosol particles. J. of Applied Meteor., 7:944-947

Kneizys, F.X., E. P. Shettle, W. O. Gallery, J. H. Chetwynd, Jr., L. W. Abreu, J.E.A. Selby, R. W. Fenn, and R. A. McClatchey, 1980: Atmospheric Transmittance/Radiance: Computer Code LOWTRAN 5. AFGL-TR-80-0067. AD A0888215

Kneizys, F. X., E. P. Shettle, W. O. Gallery, J.H. Chetwynd, Jr., L. W. Abreu, J. E. A. Selby, S. A. Clough and R. W. Fenn, 1983: Atmospheric Transmittance/Radiance: Computer Code LOWTRAN 6. AFGL-TR-83-0187 AD A137786

McElroy, J. L., 1969: A comparative study of urban and rural dispersion. J. of Appl. Meteor., 8:19-31

Pasquill, F., 1961: The estimation of the dispersion of windborne material. The Meteorological Magazine, 90:33-49

Pasquill, F., 1971: Atmospheric dispersion of pollution. Quart. J. R. Met. Soc., 97:369-395.

Radke, L. F., P. V. Hobbs, and M. W. Eltgroth, 1980: Scavenging of aerosol particles by precipitation. J. of Applied Meteor., 19:715-722.

Shettle, E. and R. Fenn, 1979: Models for the Aerosols of the Lower Atmosphere and the Effects of Humidity Variations on their Optical Properties. AFGL-TR-79-0214. Air Force Geophysics Laboratory, Hanscom AFB, MA. AD A085951

Turner, D. B., 1964: A diffusion model for an urban area. J. of Appl. Meteor., 3:83-91.

Volz, F. E., 1972: Infrared refractive index of atmospheric aerosol substances. Applied Optics, 11:755-759

REFERENCES
(Continued)

Wells, W. C., G. Gal, and M. W. Mann, 1977: Aerosol distributions in maritime air and predicted scattering coefficients in the infrared. Applied Optics, 16:654-659.

Willeke, K. and K. T. Whitby, 1975: Atmospheric aerosols: size distribution interpretation. J. of the Air Pollution Control Assoc., 25(5): 529-534.

Willeke, K., K. T. Whitby, W. E. Clark, and V. A. Marple, 1974: Size distributions of Denver aerosols--a comparison of two sites. Atmos. Env., 8:609-633.

Wolff, G. T., 1981: Particulate elemental carbon in the atmosphere. J. of the Air Poll. Control Assoc., 31:935-938.

Zib, P., 1980: Seasonal variability of the simple urban dispersion model. J. of the Air Poll. Control Assoc., 30:35-37.

APPENDIX A DEVELOPMENT OF CRITERIA FOR SELECTION OF THE URBAN AEROSOL MODEL

Diffusion theory states that the concentration of aerosols in and near an urban area is a complex function of the strength of the pollution sources, the horizontal diffusive properties of the atmosphere, the wind speed and the vertical static stability. Pasquill (1961, 1971) developed the early theory and simple graphical techniques for evaluation of downwind concentrations from a point source. The well-known Pasquill stability classifications are a part of his solution to the point source problem. Other authors (McElroy, 1969, Turner, 1964) amplified on his original development and developed more complex models of pollutant concentrations from an array of point sources. These models predict urban aerosol concentrations in large urban complexes.

Studies of measured pollution concentrations (Zib, 1980; Gifford and Hanna, 1973; Hanna, 1978) in large urban complexes have shown that the urban aerosol concentration may be estimated with reasonable accuracy using the simple formula:

$$\chi = \frac{CQ}{U} \qquad \text{(A-1)}$$

where χ is the concentration value within the urban complex, C is a dimensionless parameter, Q is the pollutant source strength in units of mass per unit area per unit time, and U is the boundary layer wind speed. An average value of C = 225 has been found to work well overall. The parameter C has been found to depend on the size of the urban area and on static stability in the boundary layer.

Gifford and Hanna (1973) defined an expression for C which depends on the distance of a point from the upwind edge of the pollutant source area. Hanna (1978) used this definition in a theoretical analysis of this parameter and its dependence on static stability. The parameter D is the distance from a point within the urban complex to its upwind edge In a large city, the expected value is one-half the characteristic diameter

Table A-1. Calculated values of C for a range of stability parameters and city sizes, D. The parameters a and b are used to model vertical dispersion. (Adapted from Hanna, 1978.)

Meteorological conditions	a	b	C for $D = 10^3$ m	C for $D = 10^4$ m	C for $D = 10^5$ m
Very unstable	0.40	0.91	41	51	63
Unstable	0.33	0.86	46	63	87
Neutral	0.22	0.80	73	115	182
Stable	0.06	0.71	341	662	1301

of the source area. He used the relation

$$\sigma_z = ax^b \qquad \text{(A-2)}$$

where σ_z, the vertical dispersion parameter, represents the effects of static stability on C. The x coordinate is measured in the direction of wind from the upwind edge of the source area. Table A-1 presents the results.

Hanna used reported values of suspended particle data for several cities to verify this theoretical values. He found an overall average value of C = 200 to be in good agreement. He also derived diurnal curves of C from observed values of carbon monoxide concentration in New Jersey, Maryland and Colorado. He showed that most of the diurnal variation in C is due to variation in static stability. He used corresponding curves of the diurnal variation in wind speed averaged for Newark, Philadelphia, Baltimore and Denver to calculate the C curves. He tested these curves by calculating concentrations of carbon monoxide in Los Angeles and comparing them to measurements. His results were as accurate overall as those from a much more complex computer simulation model.

Gifford and Hanna (1973) published pollutant concentration data for a number of American urban areas of various sizes and degrees of industrialization. We extracted a subset of these data in search of a simple method by which the user of the LOWTRAN aerosol models may evaluate the concentration of urban aerosols in an urban complex at a specified time. Table A-2 presents the data used in this analysis.

We computed the values of the source strength per unit area using the total source strength for particles and SO_x combined and the areas provided by the Department of Health, Education and Welfare (DHEW) as shown in Column 1. The resulting values of source strength per unit area are shown in Column 5.

Fig. A-1 is a plot of the average annual concentrations of particles and SO_x against the average source strength per unit area for each of the 12 urban areas listed in Table A-2. City names and area size of the pollutant sources (Column 1) are indicated at each data point. Data for all but four of the urban areas approximate a linear relationship. The four outliers are values for metropolitan areas with heavy industrialization and very large areas of pollutant sources. The two dashed lines in Fig. A-1 are drawn to approximate the relationship between pollutant concentrations and source strength. The lower line represents the relationship for small to medium sized urban areas. The upper dashed line represents the relationship for large heavily industrialized urban complexes.

These dashed lines are represented by the linear equations of the form:

$$\chi = a + bQ \qquad \text{(A-3)}$$

$$\chi = 230 + 6.2\ Q \text{ for large urban areas} \qquad \text{(A-4)}$$

$$\chi = 118 + 4.6\ Q \text{ for small to medium size cities.} \qquad \text{(A-5)}$$

The slope corresponds to the value of C/U in Eq. A-1. Using the average annual wind speed of 7.6 m sec^{-1} for large cities and 7.1 m sec^{-1} for small-medium sized cities, the resulting values of C are 47 and 32 respectively.

Eq. (A-1) requires that the linear relationship between concentration and source strength pass through the origin. Eq. (A-4) and (A-5), on the other hand, have a large y intercept. The resulting value of C is much less than that found when the form in Eq. (A-1) is used.

We assumed that values of C from Eqs. (A-4) and (A-5), were representative of neutral stability conditions. Furthermore, we assumed that an average C value of 40 would be representative for cities of all sizes under neutral stability. Using the data by Hanna in Table A-1, we estimated values of C = 20 for unstable conditions and C = 120 for stable

Fig. A-1. Average concentrations ($\mu g\ m^{-3}$) versus source strength of particles and SO_x ($\mu g\ m^{-2}\ sec^{-1}$) for selected cities. The x and y axes represent columns 5 and 3 respectively of Table A-1. Numbers in parentheses after the city names are the approximate source area sizes in Column (1) of Table 1. The dashed lines represent an approximate linear fit for the four large cities (upper line) and the eight small to medium sized cities (lower line).

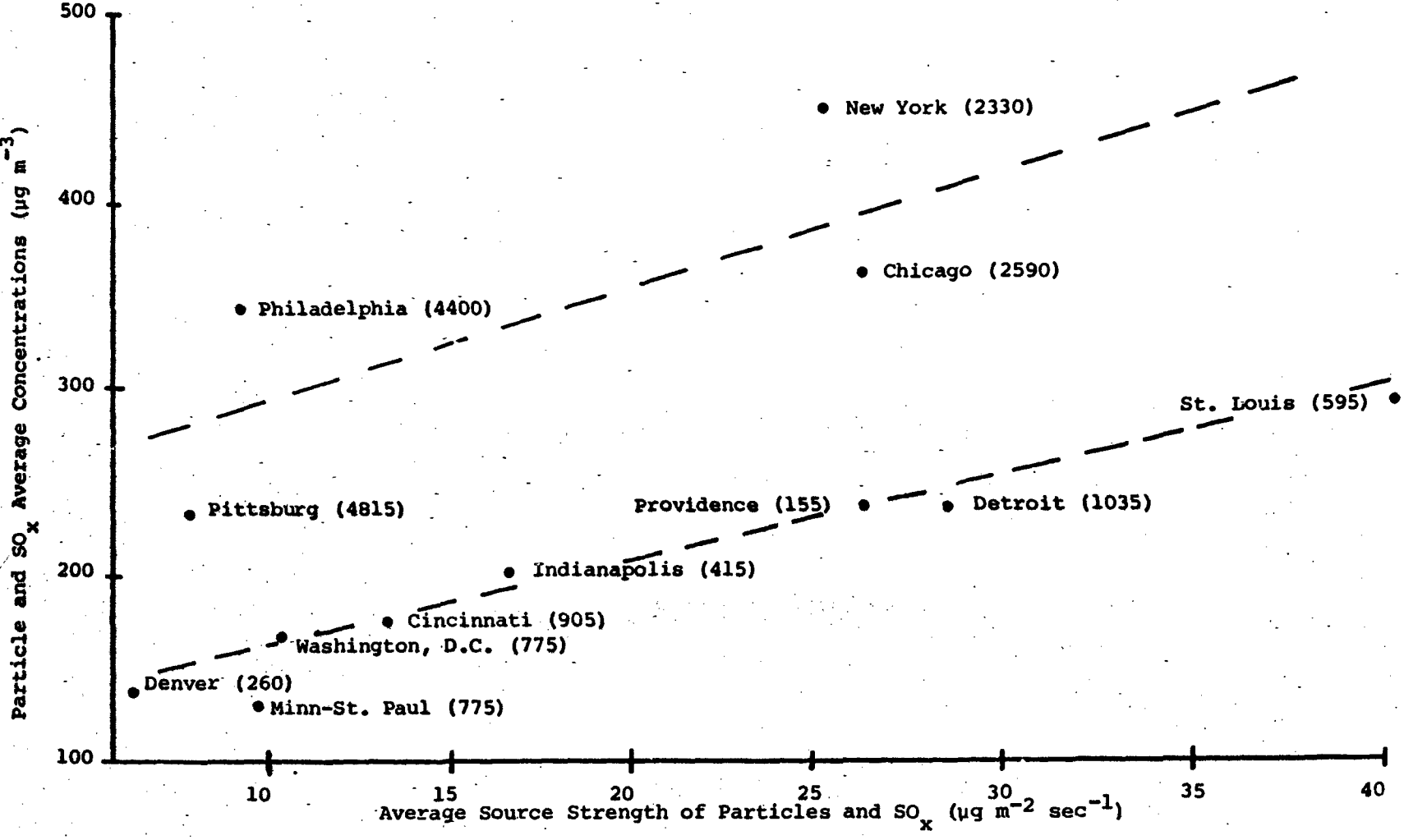

Table A-2. Source data for 12 cities used in evaluating the role of source strength and size of the urban area. Data were taken from Gifford and Hanna (1973).

City	(1)	(2)	(3)	(4)	(5)
Providence	155	141	238	8.3	26.1
Denver	260	58	135	6.3	6.4
Chicago	2590	2366	360	7.3	2[illegible].3
St. Louis	595	838	293	6.5	40.5
Philadelphia	4400	1399	341	7.8	9.1
New York	2330	2038	444	8.[illegible]	25.1
Washington, D.C.	775	282	162	[illegible].5	10.4
Detroit	1035	1026	238	7.3	28.5
Pittsburg	4815	1321	233	7.1	7.9
Cincinnati	905	422	166	6.2	13.4
Indianapolis	415	242	200	6.8	16.7
Minn. - St. Paul	775	261	132	7.5	9.7

(1) Approximate area (km^2) enclosed by an urban particulate source with strength greater than 0.1 tons day^{-1} mi^{-2}.

(2) Total average annual strength of the urban pollution sources (10^3 tons yr^{-1}). This includes both particles and SO_x emissions.

(3) Total average annual concentrations ($\mu g\ m^{-3}$). This value includes particles and SO_x concentrations.

(4) Average annual wind speed ($m\ sec^{-1}$).

(5) Q for particles and SO_x ($\mu g\ m^{-2}\ sec^{-1}$).

conditions as representative values for use in Eq. (A-3) for cities of all sizes. Since b = C/U, we may rewrite this equation in the form

$$\chi = a + \frac{C}{J} Q. \qquad \text{(A-6)}$$

If we assume that criteria for selection of the urban aerosol model in lieu of the rural model may be based on some critical value of the concentration, then the selection criteria may also be expressed in terms of the boundary layer wind speed if the stability category is defined.

We found little data on the values of pollutant concentration at which the urban aerosol model should be used. Junge (1963) cited typical values of 200-800 $\mu g\ m^{-3}$ under moderate pollution conditions. He reported concentrations as high as 4000 $\mu g\ m^{-3}$ in severe London smog. These compare to typical concentrations of 5-50 $\mu g\ m^{-3}$ for the rural background aerosol. We selected a critical value of 400 $\mu g\ m^{-3}$ as criteria for selection of the urban aerosol model. Using Eq. (A-6), the values of C described above, and the values of a in Eqs. (A-4) and (A-5), we solved for a critical value of boundary layer wind speed for each stability condition for large cities and for small to medium size cities. The resultant wind speeds provide guidance for selecting the urban aerosol model on the basis of three parameters, namely, the size and degree of industrialization of the urban area, the stability category and the forecast boundary layer wind speed. The critical wind speeds are presented in Fig. 26-D in the main body of the report.